https://doi.org/10.5194/egusphere-2026-2349
Preprint. Discussion started: 10 June 2026

Towards a process-based estimation of global lake methane emissions using LAKE2.6

Xinyu Li[1], Shushi Peng[1,2*], Victor M. Stepanenko[3,4], Liu Liu[5], Dan Zhu[1]

[1]Sino-French Institute for Earth System Science, College of Urban and Environmental Sciences, Peking University, Beijing, China
[2]Southwest United Graduate School, Kunming, China
[3]Lomonosov Moscow State University, Moscow, Russia
[4]Moscow Center of Fundamental and Applied Mathematics, Moscow, Russia
[5]Yunnan Key Laboratory of Plateau Geographical Processes and Environmental Changes, Faculty of Geography, Yunnan Normal University, Kunming, China

Correspondence to: Shushi Peng (speng@pku.edu.cn)

Abstract. While lakes play an important role in global methane (CH_4) budget, the present meta-analysis based global estimates produce large uncertainties (16.5 to 185 Tg CH_4 yr^{-1}), which were often due to lacking sufficient geographical and spatio-temporal representations. Here, we applied a one-dimensional process-based CH_4 emission model (LAKE2.6) to simulate global lake CH_4 emissions. We first calibrated the model in 10 boreal and temperate lakes and 5 tropical (24 °S–24 °N) lakes with continuous flux observations spanning 2 months to 8 years, and subsequently proposed a novel parameterization scheme for global lake CH_4 simulation based on these site-level calibrations. For global model validation, flux observations in 155 lakes from boreal and temperate regions and 21 lakes from tropical regions were collected, ranging in depth from 0.1 to 572 m and in size from 6 m^2 to 67,075 km^2. We found that simulated CH_4 fluxes in 85% of boreal and temperate lakes and 38% of tropical lakes were consistent with observations, with relative biases within ±50%. Based on these model calibration and validation results, we established a global parameterization framework and applied it to simulate global CH_4 simulations. Our estimates show that global lakes (>10 ha) emitted 17.7-20.1 Tg CH_4 yr^{-1} during the period 1979-2023. This approach improves the reliability of model extrapolations from site-level measurements to the global-scale, thus strengthening our ability to assess historical and future changes in global lake CH_4 emissions.

1 Introduction

As the second most important greenhouse gas after carbon dioxide (CO_2), methane (CH_4) has a global warming potential 27-30 times greater than that of CO_2 at a 100-year time scale, and thus its global emissions significantly drive global warming (Forster et al., 2023). While lakes occupy only 2-4% of global surface, they play a critical role in global CH_4 emissions (Pi et al., 2022; Verpoorter et al., 2014). In the recently assessment of global CH_4 budget, natural lake and ponds contributes the

https://doi.org/10.5194/egusphere-2026-2349
Preprint. Discussion started: 10 June 2026

emission of 53 Tg CH_4 yr^{-1} in 2020, accounting for ~17% of natural and indirect anthropogenic CH_4 emissions (314 Tg CH_4 yr^{-1}) (Saunois et al., 2025). However, this number was estimated with high uncertainties (22 to 151 TgCH_4 yr^{-1}) (Rosentreter et al., 2021; Johnson et al., 2022; Zhuang et al., 2023). The uncertainties hinder our ability to predict the feedback of lake CH_4 emissions to the changing climate.

The large uncertainties in estimates of global lake CH_4 emissions may partly arise from the limitations of data-driven or meta-analysis approaches (Bastviken et al., 2011; Holgerson and Raymond, 2016; Denfeld et al., 2018; Rosentreter et al., 2021). These approaches collect observed CH_4 fluxes from several lakes and then upscale them to global-scale CH_4 emissions using statistical relationships between CH_4 fluxes and lake-specific factors (such as ambient temperature, lake size, lake depth and productivity). On the one hand, the number of lakes with observed CH_4 fluxes is scarce in these studies, with only 73 to 733 lakes used to determine the statistical relationships, resulting in limited representativeness at global scale (Johnson et al., 2022). Moreover, most of the observed lakes are small (<20 km^2) and located in boreal and temperate regions, with a few lakes having continuous fluxes covering more than one month. On the other hand, the controlling factors in the statistical relationships are used to explain the spatial distribution of annual or daily CH_4 flux from lakes, leading to static estimates of global lake CH_4 emissions. Although Johnson et al. took the diel and seasonal variation of lake fluxes into consideration by multiplying scaling factors and using relationships with environmental variables (Johnson et al., 2022), studies lacking process-based consideration could not facilitate further attribution research and detect long-term changes in global lake CH_4 emissions.

Process-based models enable the estimation of long-term lake CH_4 emissions by using climate forcings as inputs and simulating dominant physical and biogeochemical processes, including CH_4 production, oxidation and transport in lakes. Due to the incomplete understanding of CH_4 production and transformations in lakes, the simulation of biogeochemical processes in a model contains several empirical parameters, which need to be calibrated against observed fluxes. This poses a challenge for global parameter calibration given the lack of spatiotemporal coverage in observed lake CH_4 fluxes. For site-level simulations, parameter calibration is typically conducted based on continuously observed data over a period of several days to months (Guseva et al., 2016; Stepanenko et al., 2016; Stepanenko et al., 2011). For global simulations, there is a trade-off between calibrating parameters in more lakes with their annual/daily mean flux and in fewer lakes with their continuous observational data, resulting in region-specific and site-specific calibrated parameters, respectively. Early efforts used the former method and directly upscaled calibrated parameters without considering temporal variations in observed fluxes and lake-specific properties (Tan et al., 2024; Zhuang et al., 2023). As lake CH_4 emissions are controlled by ecosystem productivity (Delsontro et al., 2018; Delsontro et al., 2016; Deemer et al., 2016), lake temperature (Delsontro et al., 2016; Yvon-Durocher et al., 2014), lake size and depth (Deemer and Holgerson, 2021), whether the site-specific parameters are globally representative needs careful validations. There are few process-based models to simulate global lake CH_4 emissions, compared with 16 models to simulate wetland CH_4 emissions in global CH_4 budget (Zhang et al., 2025). Zhuang et al. (2023) collected observed daily or annual mean CH_4 fluxes from just 60 lakes, calibrated a one-dimensional (1-D) model named ALBM against fluxes from 31

https://doi.org/10.5194/egusphere-2026-2349
Preprint. Discussion started: 10 June 2026

of the 60 lakes and validated the model against fluxes from the other 29 lakes. Based on the calibration and validation approach of this 1-D model, they performed a simulation of global lake CH_4 emissions with an estimate of ~24 Tg CH_4 yr^{-1} during the period 2004-2006, falling at the lower end of the range from past estimates (Zhuang et al., 2023). More model efforts are required for better estimation of lake CH_4 emissions, including the development of a new calibration approach that accounts for lake-specific properties (Tan et al., 2024).

To improve the reliability and robustness of global lake CH_4 emission using a model and further simulate emission changes in the past and future, we used a state-of-art 1-D process-based model named LAKE version 2.6 (LAKE2.6) and simulated global lake CH_4 emissions based on a new parameterization scheme. LAKE2.6 developed a module for biogeochemical processes and incorporated the dynamics of O_2, CO_2 and CH_4 in the sediment and water column, building on its previous version describing thermodynamic and hydrodynamic processes (Stepanenko et al., 2016). However, the module for CH_4 dynamics was calibrated on only a few individual lakes (Stepanenko et al., 2016; Guseva et al., 2016; Stepanenko et al., 2011). In the following sections, we collected observed CH_4 fluxes from 190 lakes and natural reservoirs (hereafter referred to as sites) regarded as a non-anthropogenic CH_4 source, including large and tropical lakes. For lakes with continuous observations, we calibrated the CH_4-related parameters of the model at the site level and proposed a new parameterization scheme based on model calibration. Then, we validated the model on other lakes with daily or annual mean observed fluxes. Finally, using the new parameterization scheme, we simulated the global CH_4 emissions from 1980 to 2023 in lakes > 0.1 km^2 across the world.

2 LAKE2.6

2.1 The model overview

LAKE model is a 1-D model that simulates the thermodynamic and hydrodynamic processes within a closed lake basin, including snow, ice, the water column and underlying sediment columns (Stepanenko, 2005; Stepanenko et al., 2011). These processes in water column are described by the 1-D vertical heat conduction equation, horizontal momentum equation and turbulence closure scheme, which are used to calculate the transport of heat and momentum (Iakunin et al., 2020). For ice and snow, the model explicitly describes heat transfer with the input of incoming radiation and liquid moisture transfer, respectively. Heat transfer in the bottom sediments is also described by the heat conduction equation, with the temperature flux at the bottom boundary set to zero (Iakunin et al., 2020). The prognostic variables from the LAKE model, such as lake temperature and ice regime, have been verified using observations in several lakes and reservoirs (Chechin et al., 2010; Iakunin et al., 2020; Stepanenko et al., 2019; Thiery et al., 2014). Furthermore, the LAKE model is widely used to assess the extent of global lake warming and phenological change in global simulation (Golub et al., 2022b; Woolway et al., 2021), participating in the lake sector of the Inter-Sectoral Impact Model Intercomparison Project (ISIMIP).

https://doi.org/10.5194/egusphere-2026-2349
Preprint. Discussion started: 10 June 2026

As an extension of the LAKE model, the LAKE2.0 model incorporates the biogeochemical module into LAKE, and a series of updated versions have been released since. The most recent version at the time of this study (LAKE2.6) was used, with subsequent updates available at http://tesla.parallel.ru/Viktor/LAKE/-/wikis/LAKE-model. Compared to the LAKE, the LAKE2.6 model includes (1) parametrizations of photosynthesis, respiration, sedimentary and biochemical oxygen demand, (2) dynamics of CO_2 and O_2, and (3) production, oxidation and transport of CH_4 (Stepanenko et al., 2016). However, among other variables, the CH_4 flux in the LAKE2.6 model has only been calibrated in a few lakes by tuning some CH_4-related parameters (Stepanenko et al., 2016; Guseva et al., 2016), with the potential of global simulations remaining unclear. We have outlined the function of CH_4-related processes in Appendix A. For a detailed description of the thermodynamic, hydrodynamic and biogeochemical processes in the LAKE2.6 model, see Stepanenko et al. (2016).

The dynamics of physical, chemical and biogeochemical processes in LAKE2.6 are simulated using vertical grid spacing in lake and sediment column, operating in a fixed time step. As shown in Figure 1, LAKE2.6 is driven by climate forcing data at each time step, including air temperature (K), atmospheric pressure (Pa), downwards shortwave and longwave radiation (W m^{-2}), wind speed (m s^{-1}), specific humidity (kg kg^{-1}) and precipitation (m). In addition, atmospheric CH_4 and CO_2 partial pressure are included in the calculation of CH_4 and CO_2 diffusion (see Appendix A for details on CH_4 diffusion) in LAKE 2.6. For static parameters, the model incorporates lake properties information, including lake area, lake depth, lake surface albedo, light extinction coefficient and CH_4-related information.

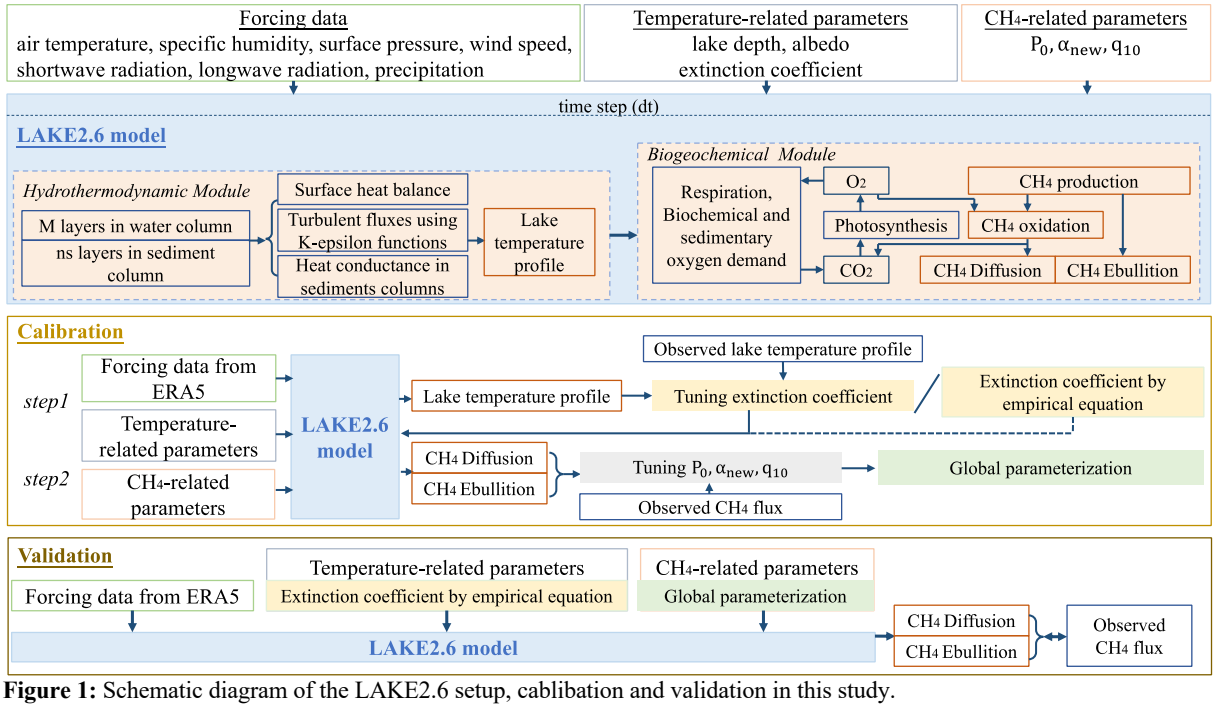

Figure 1: Schematic diagram of the LAKE2.6 setup, cablibation and validation in this study.

https://doi.org/10.5194/egusphere-2026-2349
Preprint. Discussion started: 10 June 2026

2.2 Sobol sensitivity tests

We derived 15 empirical parameters from the CH_4-related equations for model calibration (Table 1 and Appendix B). Given the overparameterization of calibrating all 15 parameters to optimize the simulated CH_4 fluxes, we decided to select several important parameters to which both diffusive and ebullitive fluxes are sensitive. In this study, we used Sobol sensitivity analysis, which is a common method to reduce the number of calibrated parameters in process-based models, to quantify the contributions of 15 parameters to the model output (Saltelli et al., 1999; Sobol′, 2001). The analysis treats the model output (Y) as the function of several independent and uniformly distributed input parameters X ($Y = f(X_1, X_2, \dots, X_n)$), and quantifies the contribution of each parameter using the first-order sensitivity index (FOSI) and total-order sensitivity index (TOSI). The $FOSI_i$ of X_i is calculated as follow:

$$FOSI_i = \frac{V_{X_i}(E_{X_{\sim i}}(Y|X_i))}{V(Y)} = 1 - \frac{E_{X_i}(V_{X_{\sim i}}(Y|X_i))}{V(Y)}, \quad (1)$$

Where $X_{\sim i}$ is the matrix of all parameters without X_i, $E_{X_{\sim i}}(Y|X_i)$ represents the mean of Y over $X_{\sim i}$ with X_i fixed and $V_{X_i}(E_{X_{\sim i}}(Y|X_i))$ represents the variance of $E_{X_{\sim i}}(Y|X_i)$ with X_i varying. Assuming X is independent, $V_{X_i}(E_{X_{\sim i}}(Y|X_i)) + E_{X_i}\left(V_{X_{\sim i}}(Y|X_i)\right) = V(Y)$ is identical in Sobol analysis and thus Eq. (1) can also be expressed as the residual part of $E_{X_i}(V_{X_{\sim i}}(Y|X_i))$. Likewise, $V_{X_{\sim i}}(E_{X_i}(Y|X_{\sim i}))$ could be considered the first-order effect of $X_{\sim i}$. $TOSI_i$ of X_i is calculated as follow:

$$TOSI_i = \frac{E_{X_{\sim i}}\left(V_{X_i}(Y|X_{\sim i})\right)}{V(Y)} = 1 - \frac{V_{X_{\sim i}}\left(E_{X_i}(Y|X_{\sim i})\right)}{V(Y)}, \quad (2)$$

We applied variance decomposition as described by Saltelli et al. (2010) to calculate the TOSI and FOSI of the 15 parameters. Both the upper and lower bounds of these parameters were derived from previous literature (Table 1) and 500 sets of parameters were generated within these bounds using Latin hypercube sampling. The sensitivities of parameters were evaluated for a random selected boreal lake with a depth of 5 meter. From Table 1, we found that both the CH_4 production rate constant (P_0) and the constant controlling the decrease in CH_4 production with sediment depth (α_{new}), which are related to CH_4 production (Appendix A and B), are the most sensitive parameters in both emission pathways, with 5% < FOSI < 47% and 33% < TOSI < 99%. This indicates that unceratinties in CH_4 production dominate uncertainties in simulated CH_4 fluxes. The following sensitive parameters are c_e and q_{10}, with 0% < FOSI < 29% and 0% < TOSI < 62%, related to ebullition and CH_4 production, respectively. Thus, P_0 and α_{new}, were selected for model calibration in this study based on their sensitivity indices. Additionally, q_{10} was also calibrated due to its similar role in CH_4 production as that of P_0 and α_{new}, as shown in Eq. (A2). Given that c_e is associated with bubble formation and showed lower sensitivity than P_0 and α_{new}, it was not included in the calibration to avoid overparameterization.

Table 1: Sensitivity analysis of parameters in the CH_4-related module of the LAKE2.6. Detailed parameter descriptions are listed in Appendix B.

https://doi.org/10.5194/egusphere-2026-2349
Preprint. Discussion started: 10 June 2026

Parameters	Units	Range	Diffusion		Ebullition		References
			FOSI	TOSI	FOSI	TOSI	
q_{10}	-	[2,6]	5.4%	15.0%	16.0%	31.1%	Yvon-Durocher et al. (2014)
P_0	mol m^{-3} s^{-1}	[1×10^{-8}-5×10^{-8}]	5.0%	98.5%	14.1%	33.1%	Stepanenko et al. (2016)
α_{new}	m^{-1}	[1,10]	11.1%	65.8%	46.5%	62.1%	Stepanenko et al. (2011); Tan et al. (2015)
$Conc_{O_2,inhib}$	ppm	[0.63,127]	0.0%	0.0%	0.0%	0.0%	Kettunen (2003)
$Decay_{O_2,exp}$	-	[1-20]	0.0%	0.0%	0.0%	0.0%	-
$Conc_{SO_4,inhib}$	µmol L^{-1}	[0-100]	0.0%	0.0%	0.0%	0.0%	Lovley and Klug (1986)
$Decay_{SO_4,exp}$	-	[1-20]	0.0%	0.0%	0.0%	0.0%	-
methox2sod	%	[0,64]	0.0%	0.0%	0.0%	0.0%	Liikanen et al. (2002)
$K_{CH_4,w}$	mol m^{-3}	[0.001-0.0662]	0.1%	0.0%	0.0%	0.0%	Tan et al. (2015)
$K_{O_2,w}$	mol m^{-3} s^{-1}	[0.001,0.2]	5.9%	11.4%	0.0%	0.0%	Tan et al. (2015)
$V_{max,w}$	mol m^{-3} s^{-1}	[1×10^{-8},1×10^{-4}]	0.3%	0.3%	0.0%	0.0%	Tan et al. (2015)
c_e	s^{-1}	[2.78×10^{-4},0.113]	28.6%	61.9%	0.0%	0.0%	Tan et al. (2015)
α_e	-	[0.2,0.6]	0.0%	0.0%	0.0%	0.0%	-
$Intercept_{bubble}$	%	[80,99]	1.5%	1.8%	3.1%	1.9%	-
$Intercept_{bubble}$	%	[50,70]	0.0%	0.0%	0.0%	0.0%	Greene et al. (2014); Tan et al. (2015)

2.3 Time step and vertical spacing

For parameters related to temporal and vertical grid spacing, including the time step (Δt), the number of layers in the water column（M), the number of layers in the sediment column（ns) and the sediment depth, higher resolution generally improves model accuracy but increases computational cost. To balance the accuracy and computational efficiency, we conducted a separate sensitivity analysis for each parameter. Specifically, we first ran the LAKE2.6 model for a lake with a mean water depth of 5 m using climate data from 1979 across three climate regions （60 °N–90 °N, 30 °N–60 °N and 30 °S–30 °N) to determine the optimal sediment depth. We next ran simulations for a lake with both mean water depth and sediment depth of 5 m to determine optimal values of M, ns and Δt . We hypothesized that a sediment depth of 1 m provides the best performance for a lake with water depth of 5 m. We further hypothesized that a Δt of 10 seconds, M of 50 layers and ns of 45 layers provide best performance for a lake with water depth and sediment depth of 5 m. By tuning M, ns, Δt and sediment depth individually, we compared the simulated daily mean water temperature, ebullitive and diffusive CH_4 fluxes to determine the optimal values. Taylor diagrams were used to present the sensitivity of model to these parameters in terms of standard deviation, correlation coefficient (R) and root mean square error (Figs. S1-S4 in the Supplement). Based on the diagrams, we set Δt to 60 s, which shows a good agreement with the simulation using a 10-s time step (R > 0.9; Fig. S1 in the Supplement). M could be set to 2-10 layers per meter and ns could be set to 3 layers per meter (Figs. S2–S3 in the Supplement). The sediment depth could be set to 20%–100% of the lake depth (Fig. S4 in the Supplement). To balance model accuracy and computational cost when using finer vertical resolution, we set M to 10 layers per meter for lakes shallower than 10 m, 5 layers per meter for lakes with

https://doi.org/10.5194/egusphere-2026-2349
Preprint. Discussion started: 10 June 2026

depths of 10-25 m and 2 layers per meter for lakes deeper than 25 m. The sediment depth in the model was set to one-third of the lake depth, with ns set to 3 layers per meter in sediment depth.

3 Data compilation and model setup

3.1 Data compilation

3.1.1 Continuous CH_4 fluxes

We synthesized 10 sites with continuous total CH_4 flux observations ranging from 2 months to 8 years, with surface area ranging 0.011–38 km^2, mean depth ranging 0.7–7 m and max depth ranging 1.3–25 m (Fig. 2a and Table 2). Of these lakes, Mellersta Harrsjön (MH), Inre Harrsjön (IH), Villasjön (VS), Lake Tämnaren, Lake Toolik and Lake Kuivajärvi are sub-arctic and boreal lakes (>50 °N) located in North America and Europe, while the other four lakes (Lake Dagow, Lake Suwa, Trout Bog and Lake Acton) are temperate lakes located in North America, Europe and Asia (Fig. 2a). The 10 sites cover a wide range of lake productivity, from oligotrophic to eutrophic. Specifically, MH, IH, VS, and Tämnaren are four Swedish lakes, with MH, IH and VS having high organic carbon input from surrounding fens, streams, and springs and Lake Tämnaren having high turbidity from surrounding agricultural fields (Jansen et al., 2019). Lake Toolik is an oligotrophic lake surrounded by small shrubs and tundra (Macintyre et al., 2009). Lake Kuivajärvi and Trout Bog are two humic lakes within the managed forests in Finland and the United States, respectively (Gorsky et al., 2021; Erkkila et al., 2018). Lake Dagow and Lake Suwa are two eutrophic lakes which are of glacial origin in Germany and of tectonic origin in Japan, respectively (Casper, 2012). Lake Acton is a eutrophic reservoir, which is also included in this study and regarded as a non-anthropogenic CH_4 source similar to natural lakes (Waldo et al., 2021). For MH, IH and VS, the observed CH_4 diffusive fluxes (Jansen et al., 2020c) and ebullitive fluxes (Wik et al., 2013; Jansen et al., 2020b; Wik et al., 2020) were obtained from the Bolin Centre Database (https://bolin.su.se/data/). The observed CH_4 total fluxes were obtained from AmeriFlux (https://ameriflux.lbl.gov/data/download-data/, last access: 4 April 2026) for Lake Acton and Lake Trout Bog, and from FLUXNET-CH4 database (https://fluxnet.org/data/download-data/, last access: 4 April 2026) for Lake Dagow and Lake Suwa. The observed CH_4 total fluxes for Lake Tämnaren, Lake Toolik and Lake Kuivajärvi were obtained from the Environmental Data Initiative (https://portal.edirepository.org/nis/mapbrowse?packageid=edi.835.1) (Golub et al., 2023),

For MH, IH and VS, long-term CH_4 observations covering the open-water period (May-October) from 2009 to 2017 include both ebullitive and diffusive fluxes, following the methods described by Wik et al. (2013) and Bastviken et al. (2004), respectively. In brief, ebullitive fluxes are calculated based on the mass of CH_4 gas which is collected by bubble traps during deployment periods of 24–72 h and then analysed using a gas chromatograph (Wik et al., 2013). A total of 40 bubble traps were deployed across different depth zones in three lakes (n = 13 in MH, n = 17 in IH and n = 10 in VS), measuring 14676

https://doi.org/10.5194/egusphere-2026-2349
Preprint. Discussion started: 10 June 2026

ebullitive fluxes from June to October during the period 2009–2017 (Jansen et al., 2019). Diffusive fluxes are estimated based on the CH_4 concentration difference between lake water and air, which are collected in floating chambers at regular intervals (2-4 times) within 24 h (Bastviken et al., 2004; Jansen et al., 2019). A total of 10 floating chambers were deployed in three lakes, with four deployed in each lake of MH and IH and two in VS, conducting 1306 measurements about every week between May and October in 2010–2017 (Jansen et al., 2019). In this study, we compiled a total of 22-24 months with available monthly fluxes for ebullition across the three lakes, and 16–17 months for diffusive flux. Specifically, daily ebullitive fluxes for each lake are averages of measurements from all bubble traps over the course of a day based on the deployment periods of the traps. Monthly ebullitive fluxes are the sum of daily fluxes covering >25 days for each month. For diffusion, daily diffusive fluxes for each lake are calculated as the averages of measurements from all floating chambers in a day. Monthly diffusive fluxes are the product of the number of days in a month and the mean daily fluxes when the number of available measurements is >25 for the month.

For the other seven lakes, continuous total CH_4 fluxes are measured by eddy covariance (EC) flux towers, which rely on the equipment of infrared gas analyzers to measure air density, sonic anemometers to measure wind speed and direction, and thermometers to measure water temperature (Deemer et al., 2016). Across the seven sites, the EC systems are located at different heights either on the shore or on a raft or buoy in the lake, recording half-hourly CH_4 fluxes over a period of 1 to 4 years, without distinguishing between diffusion and ebullition (Erkkila et al., 2018; Golub et al., 2023; Delwiche et al., 2021; Waldo et al., 2021) (Table 2). Given the gaps in raw data from EC systems, we only used available fluxes for >6 h per day (available day) and >10 available days to calculate daily and monthly CH_4 fluxes for each lake site, respectively. Besides raw data, half-hourly gap-filling data using artificial neural network (ANN) is included for Lake Dagow and Lake Suwa derived from FLUXNET-CH_4 (Waldo et al., 2021). We compared daily CH_4 flux from the gap-filling data and raw data for each lake, finding a great agreement for Lake Dagow but not for Lake Suwa. Daily and monthly CH_4 fluxes for Lake Dagow were calculated using ANN data, requiring complete 24-h data coverage for daily estimates and >28 available days per month for monthly estimates, respectively (Fig. S5 in the Supplement). Using data derived from EC systems, we compiled data for monthly CH_4 fluxes across seven lakes, ranging from 2 to 32 months of availability.

https://doi.org/10.5194/egusphere-2026-2349
Preprint. Discussion started: 10 June 2026

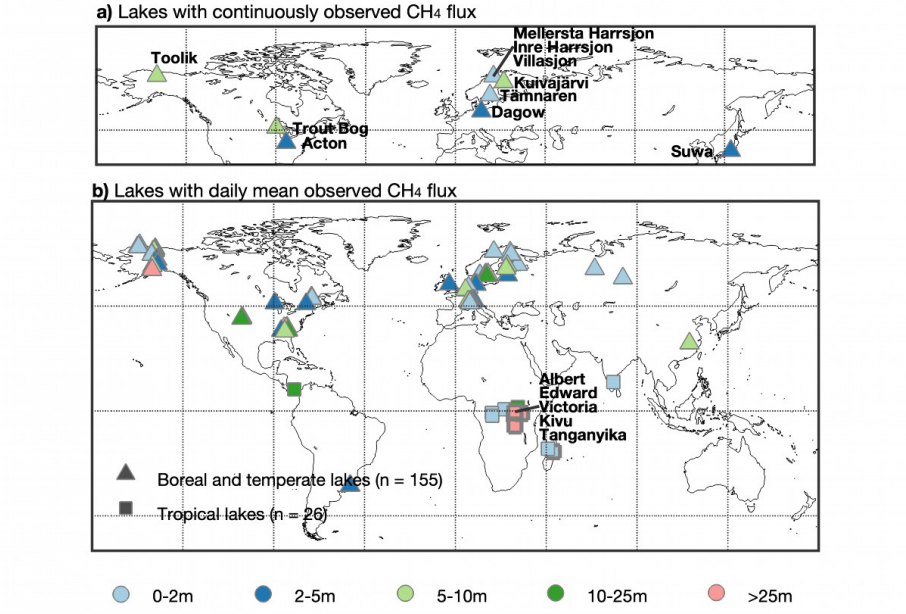

Figure 2: The distribution of sites used in this study. (**a**) Sites with continuously observed CH_4 fluxes. (**b**) Sites with daily mean observed CH_4 fluxes. Triangles and rectangles represent boreal and temperate sites (n = 165) and tropical sites (n = 26), respectively. Bold rectangles represent tropical sites with CH_4 fluxes averaged from continuous measurement (n = 5). Together with 10 other sites with continuously observed CH_4 fluxes in panel (**a**), these lakes (n = 15 in total, shown in bold text) were used for model calibration, while the remaining lakes (with daily mean fluxes) were used for model validation. Different colors represent the depth zones of the lakes.

Table 2: The lake properties, CH_4 measurement periods, and lake temperature measurement periods of 15 lakes used for model calibration.

Site name	Surface area (km^2)	Mean depth (m)	Max depth (m)	Country	CH_4 measurement period	Lake temperature measurement period
Mellersta Harrsjön	0.011	1.9	6.7	Sweden	2010-2017, May-Oct (Diffusion) 2009-2017, June-Oct (Ebullition)	2009-2019
Inre Harrsjön	0.023	2	5.2	Sweden	2010-2017, May-Oct (Diffusion) 2009-2017, June-Oct (Ebullition)	2009-2019
Villasjön	0.17	0.7	1.3	Sweden	2010-2017, May-Oct (Diffusion) 2009-2017, June-Oct (Ebullition)	2010-2019
Lake Tämnaren	38	1.3	2	Sweden	2010.9.13-2012.9.13	-
Lake Toolik	1.5	7	25	USA	2012.6.12-2012.8.21	-
Lake Kuivajärvi	0.62	6.3	13.2	Finland	2012.9.2-2015.9.22	2012-2023
Lake Dagow	0.24	5.0	9.5	Germany	2015.1.1-2018.12.31	-
Lake Suwa	2	4.6	6.8	Japan	2016.6.4-2016.12.31	-
Trout Bog	0.011	5.6	7.9	America	2020.3.27-2020.10.28	2003-2014
Lake Acton	2.4	3.9	8	America	2017.2.1-2018.11.13	2010-2014
Lake Edward	2253	33	117	DR Congo; Uganda	2016.10.20-11.4;2017.3.23-3.31; 2018.1.18-2.2; 2019.3.21-3.30	-

https://doi.org/10.5194/egusphere-2026-2349
Preprint. Discussion started: 10 June 2026

Lake Victoria	67075	40	79	Congo; Uganda	2018.3.29-4.8; 2018.10.25-11.4;2019.6.7-6.17	-
Lake Tanganyika	32821	572	1470	DR Congo; Tanzania; Zambia; Burundi	2019.10.8-10.18; 2021.5.1-5.7	-
Lake Albert	5402	25	58	Uganda; DR Congo	2019.6.20-6.23	-
Lake Kivu	2371	240	485	DR Congo; Rwanda	2007.3.15-3.29;2007.8.28-9.10;2008.6.21-7.3; 2009.4.21-5.5; 2010.10.19-10.27	-

3.1.2 Daily mean lake CH_4 fluxes

We used a dataset compiled by Rosentreter et al. (2021) which includes daily mean diffusive, ebullitive, or total CH_4 fluxes from 313 sites (including 86 reservoirs) and covers data up to May 2019. Lake latitude, longitude and properties such as surface area, mean depth, and max depth are also included in this dataset. We only used sites (n = 233) with available surface area and mean depth, or where mean depth could be obtained from other online studies focusing on these sites. Of the 233 sites, we excluded 4 lakes (Lake Tämnaren, Lake Toolik and Lake Kuivajärvi and VS) with continuous CH_4 flux as described above, 10 thermokarst lakes not considered in this study, 2 lakes where ebullition measured at the sediment, and 1 lake where ebullition measured by echosounder, which may be biased by non-bubble acoustic targets (Delsontro et al., 2015). For 66 reservoirs of the 233 sites, we excluded 47 reservoirs due to their anthropogenic CH_4 emission including emissions after impoundment and during water-level drawdowns, 8 floodplains with high variations in water level which could be categorized as wetlands, 1 reservoir with a total flux of zero and 3 reservoirs where the studies focused on CH_4 emission from flooding experiments. Finally, a total of 157 sites (including 7 non-anthropogenic reservoirs) were included in this study, with total flux expressed as mean flux over <10 days of discontinuous measurements over the period, ranging 0.4–1845.2 mg CH_4 m^{-2} day^{-1}. The ebullitive fluxes were obtained using chambers, funnel traps or lake ice ebullition surveys, while the diffusive fluxes were obtained using chambers or calculated from dissolved CH_4 concentrations in surface water based on Fick's law. Most sites are situated in subarctic, boreal and temperate regions in the Northern Hemisphere (n = 155; Fig. 2b), with only two sites located in the tropical region.

To reduce the geographic bias of lakes with observed CH_4 fluxes, we included tropical lakes by using a dataset compiled by Borges et al. (2022), which provides observed CH_4 fluxes in 24 African lakes. These lakes have a wide range of mean depth, from 0.1 m to 572 m, with 6 out of 24 lakes deeper than 25 m, and they occupy ~49% of the lake surface area in Africa, including African Great Lakes (AGL) such as Lake Edward, Lake Victoria, Lake Kivu and Lake Tanganyika. The diffusive CH_4 fluxes of the 24 lakes were calculated from CH_4 concentrations measured at one or several locations, depending on lake

https://doi.org/10.5194/egusphere-2026-2349
Preprint. Discussion started: 10 June 2026

size, over 1–55 days between 2007 and 2021 based on Fick's law. As the ebullitive fluxes were only measured in the littoral zones without considering the different depth zones, we omitted the ebullitive fluxes measured in 4 of the 24 lakes and only considered the diffusive fluxes in all 24 lakes. Combining with the two lakes from Rosentreter et al. (2021), a total of 26 tropical lakes with diffusive fluxes are included in this study (Fig. 2b). Among the 26 lakes, it is noteworthy that the diffusive fluxes in 5 lakes (including the four AGL mentioned above) are averages from >3 days of continuous measurements.

3.1.3 Ancillary Data

We collected observed temperature profiles for lakes with continuous CH_4 flux observations which include 10 boreal and temperate lakes and 5 tropical lakes (Fig. 2). Observed temperature profiles were available for 5 of 15 lakes including Lake MH, IH, VS, Trout Bog and Lake Acton. Data for the first three lakes were obtained from the repository site of the Bolin Centre for Climate Research at Stockholm University (https://bolin.su.se/data), while data for Trout Bog and Lake Acton were from North Temperate Lakes Long-Term Ecological Research Program (https://portal.edirepository.org/nis/home.jsp). Temperature profiles were measured at the deepest zone of the lakes at every 5–15 min and at the depth intervals of 0.2–1 m, covering the period from 2009 to 2019 for Lake MH, IH and VS, from 2003 to 2014 for Trout Bog and from 2010 to 2014 for Lake Acton (Table 2). To extract temperature information for five tropical lakes without available observed temperature profiles, we used lake-wide mean surface temperature data from the Along Track Scanning Radiometer (ATSR) Reprocessing for Climate: Lake Surface Water Temperature and Ice Cover (ARC-Lake) dataset (www.laketemp.net) (Maccallum and Merchant, 2012; Layden et al., 2015), which includes daily satellite-derived data from 1995 to 2012.

In this study, we used LAKE2.6 to simulate CH_4 fluxes at 191 sites (Fig. 2) for model calibration and validation, and subsequently conducted a global simulation to estimate global lake CH_4 emissions. To drive the model, we used hourly climate forcing data from European Centre for Medium Range Weather Forecasts (ECMWF) ERA5, covering the period 1979-2023, with a spatial resolution of $0.25° \times 0.25°$. The lake geographical location and properties for global simulation are from a widely used database named HydroLAKES, which includes more than 1.4 million water bodies (including 6687 reservoirs) larger than 10 ha (Messager et al., 2016). We also used annually averaged global atmospheric CO_2 and CH_4 concentration from 1979 to 2023 for global simulation derived from NOAA Global Monitoring Laboratory measurement (https://gml.noaa.gov/ccgg/trends_ch4/).

3.2 Model setup for calibration and validation

We calibrated the model using CH_4 fluxes from 10 boreal and temperate lakes with continuous observations and from 5 tropical lakes with mean fluxes averaged from continuous measurements (Fig. 2). The model was validated using fluxes averaged from discontinuous measurements in 155 boreal and temperate lakes, as well as 21 tropical lakes. For calibration and validation, the

https://doi.org/10.5194/egusphere-2026-2349
Preprint. Discussion started: 10 June 2026

forcing data for each lake is extracted based on its observation location, from January of the year preceding the earliest observed year to December of the latest observed year.

A spin-up simulation was conducted prior to model calibration and validation to ensure that the model reaches equilibrium in both the water and sediment columns, with the time required to reaches equilibrium depending on lake depth, which determines M and ns in LAKE2.6 (Figs. S2–3 in the Supplement). We conducted a 1000-year simulation with cycled one-year climate forcing (1979) for lakes ranging from 1 to 800 m in depth and determined the spinup period for the annual CH_4 diffusion emission, ebullition emissions and annual mean temperature averaged over the whole lake column with default CH_4-related parameters. As shown in Figs. S6–S7 in the Supplement, we set a 30-year spinup period for lakes shallower than 30 m, a 60-year spinup period for lakes with the depth between 30 and 60 m, a 100-year spinup period for lakes with the depths between 60–100 m and a 700-year spinup period for lakes of other depths (Figs. S6–7 in the Supplement). After reaching equilibrium, we found that the annual CH_4 flux declines with increasing lake depth, and plateaus once lake depth exceeds 100 m (Fig. 3).

The simulation processes for calibration and validation are shown in Fig. 1. Specifically, given that the light extinction coefficient is an important parameter in determining simulated lake temperature profiles in previous studies (Thiery et al., 2014; Heiskanen et al., 2015), we first tuned the light extinction coefficient by comparing the simulated and observed daily lake temperature profiles for sites with observations. For lakes without observations, we used the empirical equation from Håkanson to calculate the light extinction coefficient based on lake mean depth (Håkanson, 1995). We next tuned q_{10}, P_0 and α_{new} at 10 sites by minimizing discrepancies between simulated and observed CH_4 fluxes at monthly and annual scales based on the root mean square error (RMSE) and obtained ranges of optimal parameters. Based on 10 sets of optimal site-specific parameters that represent the performance of LAKE2.6 in boreal and temperate lakes, we established a relationship linking the three CH_4-related parameters and lake properties. These relationships were then applied at 5 tropical lakes and adjusted α_{new} due to large and deep tropical lakes used here (see section 4.3). Considering that the mean observations averaged from limited continuous measurements (4–66 days) for the 5 lakes could not be accurately captured by the model due to the stochasticity of CH_4 emissions, we compared the observed fluxes with the simulated fluxes selected as the closest values to the observations within a ±30-day window around each observation date. After calibration, the parameterizations of CH_4-related processes in LAKE2.6 were established for all global lakes.

For model validation, we simulated the daily mean CH_4 fluxes using light extinction coefficient calculated from the empirical equation of Håkanson (1995) and CH_4-related parameters calculated from the established relationships. Following the same approach used for model calibration in tropical lakes, the simulated fluxes were extracted as the values closest to the observations within a ±30-day window for each observation date.

https://doi.org/10.5194/egusphere-2026-2349
Preprint. Discussion started: 10 June 2026

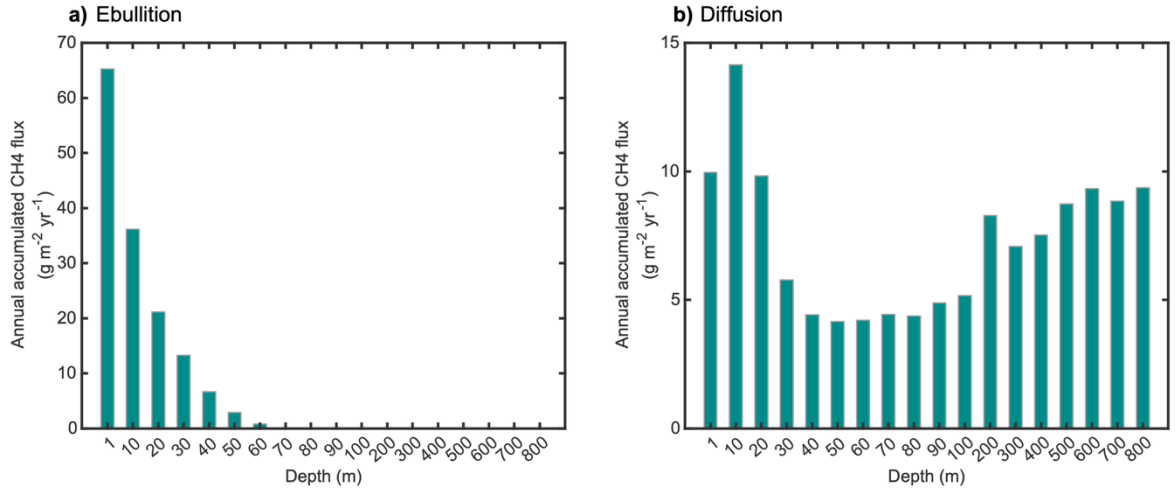

Figure 3: Equilibrium annual accumulated CH_4 emissions in lakes with increasing depths simulated by LAKE2.6 under the climate forcing of 1979, including (**a**) ebullition and (**b**) diffusion.

4 Model calibration

4.1 Model calibration in lakes with continuous CH_4 flux

Following model calibration by tuning the light extinction coefficient in 5 lakes with observed temperature profile and subsequently tuning CH_4-related parameters at monthly and annual time scales, Figs. 4–6 show the comparison between simulated and observed temporal changes in CH_4 flux for 10 boreal and temperate lakes using LAKE 2.6.

For MH, IH and VS with multiyear measurements of lake temperature profiles and CH_4 emissions in two pathways, the model was able to reproduce the seasonal cycle of lake temperature (Figs. S8–10 in the Supplement) and capture the magnitude of both monthly and annual accumulated CH_4 emission (Fig. 4). For ebullition which is the dominant CH_4 emission pathway in the three lakes, the mean monthly flux in Lake MH, IH and VS is 547, 245 and 971 mg CH_4 m^{-2} mon^{-1} from observations, and 551, 217 and 966 mg CH_4 m^{-2} mon^{-1} from simulations, respectively. By adding the available monthly observations and corresponding simulations to the annual accumulated flux, the mean annual ebullitive flux in MH, IH and VS is 1459, 654 and 2670 mgCH_4 m^{-2} yr^{-1} from observations and 1468, 580 and 2657 mg CH_4 m^{-2} yr^{-1} from simulations. For diffusion, the mean monthly flux in Lake MH, IH and VS is 265, 204 and 188 mg CH_4 m^{-2} mon^{-1} from observations and 244, 208 and 277 mg CH_4 m^{-2} mon^{-1} from simulations. The mean annual diffusive flux is 531, 434 and 375 mg CH_4 m^{-2} yr^{-1} from observations, and 488, 442 and 555 mgCH_4 m^{-2} yr^{-1} from simulations. However, LAKE2.6 could not simulate ebullition events with comparably high fluxes, which might be due to the uncertain mechanism of the pulse of CH_4 emissions, for example the neglect of water level effects on ebullition (Tan et al., 2024; Tan et al., 2015). Nevertheless, the model showed a better agreement in episodic ebullition than in diffusion for the three lakes. For example, the RMSE between observed and simulated monthly CH_4 ebullitive

https://doi.org/10.5194/egusphere-2026-2349
Preprint. Discussion started: 10 June 2026

flux in Lake MH, IH and VS is 353, 158 and 415 mg CH_4 m^{-2} yr^{-1}, accounting for 16–24% of the mean monthly flux, while the RMSE for monthly CH_4 diffusive flux is 29–66% of the mean monthly flux. This could result from the setting that lake emits CH_4 immediately after ice breakup, leading to deviations of diffusive fluxes between the simulation and observation occurring more frequently in the months after ice breakup (Fig. 4a-i).

Of the remaining 7 lakes, Lake Tämnaren, Lake Kuivajärvi, Lake Dagow and Lake Acton have multiyear measurements of total CH_4 flux covering 2–4 years (Fig. 5), while Lake Toolik, Lake Suwa and Trout Bog have continuous measurements covering 2–5 months (Fig. 6). We tuned the light extinction coefficients in Lake Acton, Lake Kuivajärvi and Trout Bog using observed temperature profiles (Figs. S11–13 in the Supplement) and calculated the light extinction coefficients for the other 4 lakes. After tuning the CH_4-related parameters, LAKE2.6 was able to simulate the magnitude of monthly total CH_4 flux for all the 7 lakes. Specifically, the mean monthly total CH_4 flux for Lake Tämnaren, Lake Kuivajärvi, Lake Dagow, Lake Acton, Lake Toolik, Lake Suwa and Trout Bog was 846, 24, 965, 3409, 100, 7786 and 174 mg CH_4 m^{-2} mon^{-1} for observations, and 826, 32, 1329, 3816, 101, 7544 and 171 mg CH_4 m^{-2} mon^{-1} for simulations, respectively. The model could reproduce the seasonal cycle of total CH_4 flux for Lake Kuivajärvi, Lake Dagow and Lake Acton in years with more than 9 months of observations, including 2013 and 2015 for Lake Kuivajärvi, 2016 and 2017 for Lake Dagow, and 2017 and 2018 for Lake Acton (Fig. 5c, d, g). At the annual scale, the model could simulate a similar magnitude of mean annual accumulated total CH_4 flux for lakes with both multiyear observations (Fig. 5) and one-year observations (Fig. 6). As a result, the similar magnitudes of monthly CH_4 fluxes between simulations and observations across the 10 lakes indicate that LAKE2.6 can reproduce the magnitude of CH_4 fluxes in boreal and temperate lakes.

https://doi.org/10.5194/egusphere-2026-2349
Preprint. Discussion started: 10 June 2026

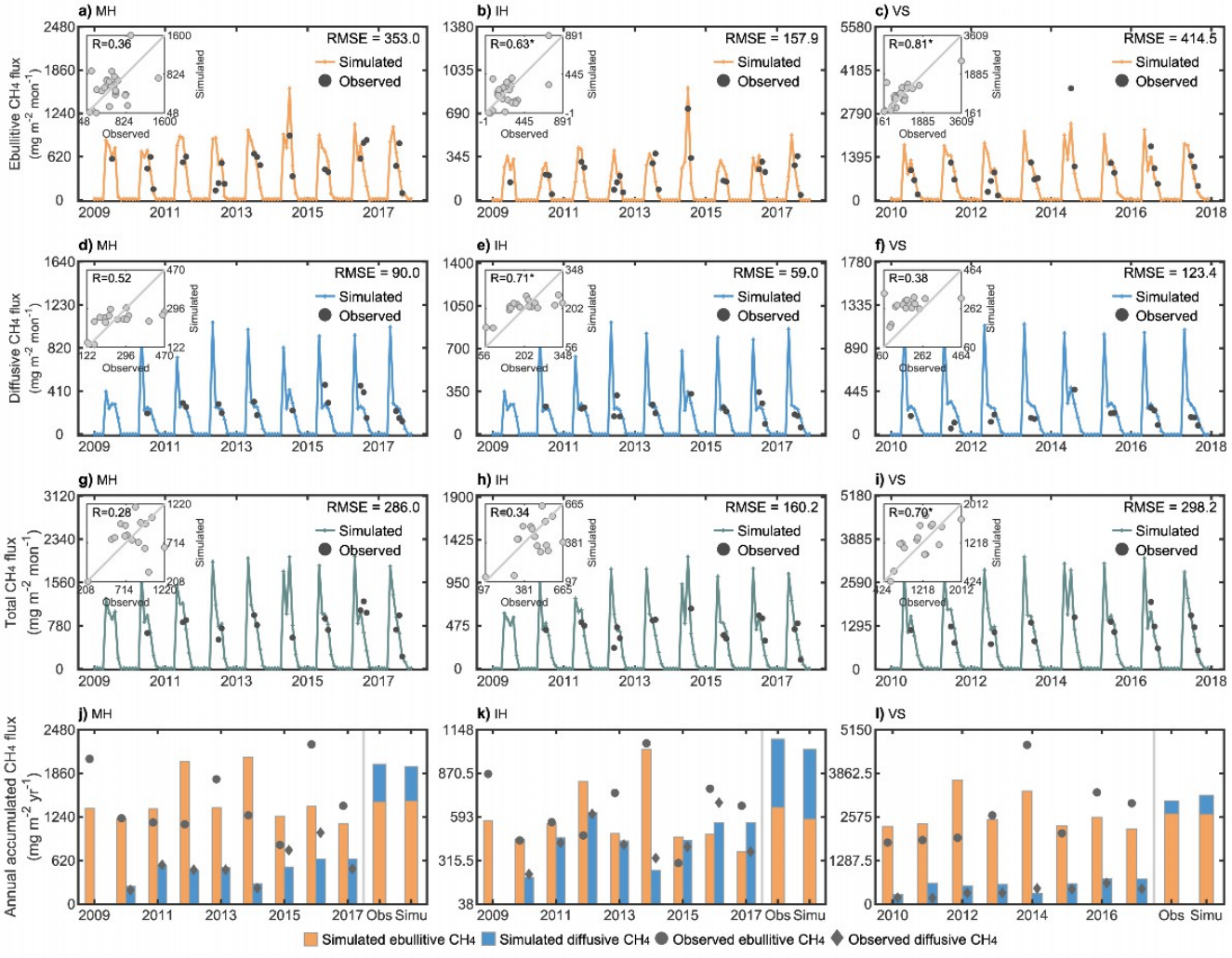

Figure 4: Performance of LAKE2.6 in simulating monthly and annual accumulated CH_4 fluxes in Mellersta Harrsjön (MH), Inre Harrsjön (IH) and Villasjön (VS). (**a**–**i**) Comparison of monthly ebullitive CH_4 fluxes (**a**–**c**), diffusive CH_4 fluxes (**d**–**f**) and total CH_4 fluxes (**g**–**i**) between simulation and observation for MH (left column), IH (middle column) and VS (right column), respectively. The insets in panels (**a**–**i**) show scatter plots between simulated and observed fluxes, and * indicates $p < 0.01$. (**j**–**l**) Comparison of annual accumulated diffusive and ebullitive CH_4 in MH (**j**), IH (**k**) and VS (**l**). In each panel, the left side shows the comparison for annual fluxes and the right side shows the comparison for mean annual CH_4 fluxes, including ebullition and diffusion.

https://doi.org/10.5194/egusphere-2026-2349
Preprint. Discussion started: 10 June 2026

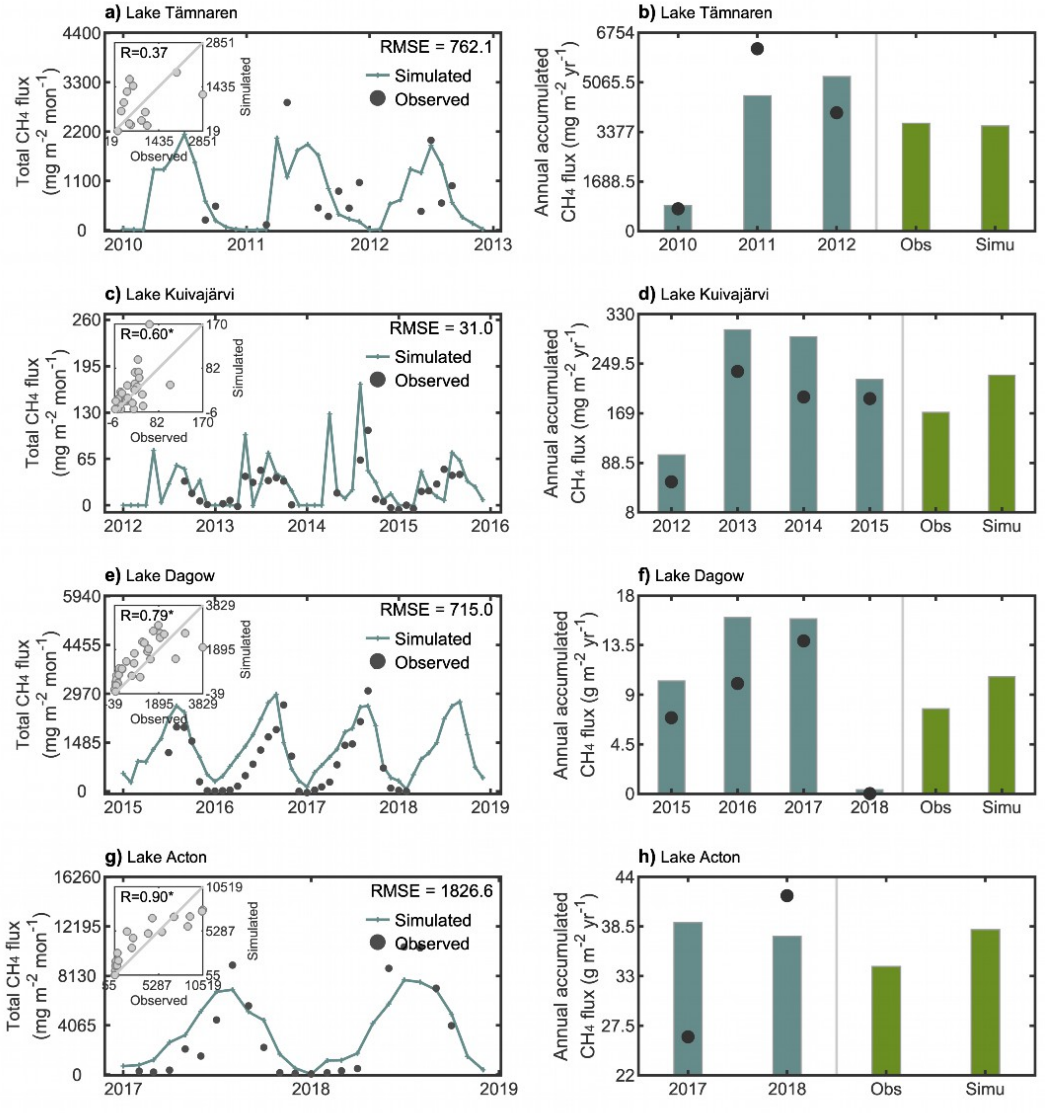

Figure 5: Performance of LAKE2.6 in simulating monthly and annual accumulated total CH_4 fluxes in Lake Tämnaren (**a**, **b**), Lake Kuivajärvi (**c**, **d**), Lake Dagow (**e**, **f**) and Lake Acton (**g**, **h**). The first column shows comparisons between simulated and observed monthly total CH_4, with insets showing corresponding scatter plots and * indicating $p < 0.01$. The second column shows the comparisons of annual accumulated total CH_4 fluxes (left side) and mean annual fluxes (right side). In the left side, the dark green bars represent simulated fluxes and dots represent observations.

https://doi.org/10.5194/egusphere-2026-2349
Preprint. Discussion started: 10 June 2026

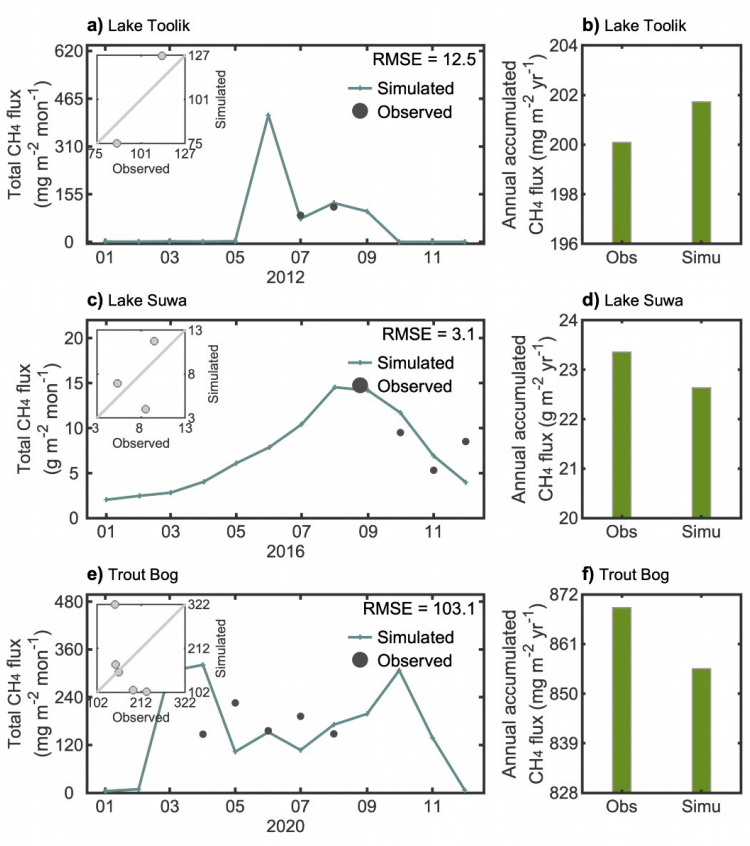

370 **Figure 6:** Same as Fig. 5, but showing the performance of LAKE2.6 in simulating monthly total CH_4 fluxes (left column) and annual accumulated CH_4 fluxes (right column) for Lake Toolik (**a**, **b**), Lake Suwa (**c**, **d**) and Trout Bog (**e**, **f**).

4.2 Spatial variation of calibrated parameters

After model calibration in in terms of water turbidity, P_0 and α_{new} were tuned within site-specific ranges while q_{10} was set to 2.5 across 10 lakes (Table S1 in the Supplement), consistent with Eq. (A2) in which CH_4 production rate increases with
375 increasing P_0 and q_{10} but decreases with increasing α_{new}. The variability in P_0 and α_{new} across the 10 lakes, which control the quality of substrates in sediments and the vertical pattern in available substrates, respectively, suggests that site-level definition of P_0 and α_{new} are essential for accurately simulating CH_4 emissions from global lakes (Walter and Heimann, 2000). Given that climate variables and morphometric properties (such as lake depth and area) influence the quantity and quality of substrates (Gudasz et al., 2010), the differences in P_0 and α_{new} across these lakes could be related to the lake-specific
380 properties. Since q_{10} represents the temperature dependence of CH_4 production, which is observed to be similar across different climate gradients in lake sediment incubations (Walter and Heimann, 2000; Gudasz et al., 2010), we followed the calibration results and hypothesised that a universal q_{10} value of 2.5 applies to all global lakes.

https://doi.org/10.5194/egusphere-2026-2349
Preprint. Discussion started: 10 June 2026

Given that P_0 in high-latitude lakes is set higher than in other lakes (Table S1 in the Supplement), we suggest that site-specific climate conditions may influence the value of P_0 for 10 lakes. We used the mean air temperature during the ice-free months from 1980 to 2023 derived from ERA5 to represent the warm-season climate, and identified a relationship between the ranges of P_0 and air temperature (Fig. 7a, $R^2 = 0.45$, $p < 0.1$). This indicates that lakes with higher temperature tend to have lower CH_4 production potential due to lower organic carbon concentration in sediment (i.e., higher temperature lake generally has lower concentration of organic carbon in sediment; see section 7.1). Note that, this relationship is based on data from 9 lakes excluding Lake Suwa, where the P_0 was tuned using observed CH_4 flux from September to December, a period with lower temperature than the ice-free period. Additionally, we considered different combinations of morphometric properties to represent α_{new} for each lake. We found a negative relationship between α_{new} and the product of air temperature and the logarithmic ratio of effective lake radius to mean depth ($lg(\sqrt{lake\ area}/depth/\sqrt{\pi})$, Fig. 7b), suggesting that larger and shallower lakes show higher CH_4 production rates at a constant temperature. Based on these relationships, we could upscale P_0 and α_{new} from the 10 lakes to other boreal and temperate lakes (30–90 °N or °S).

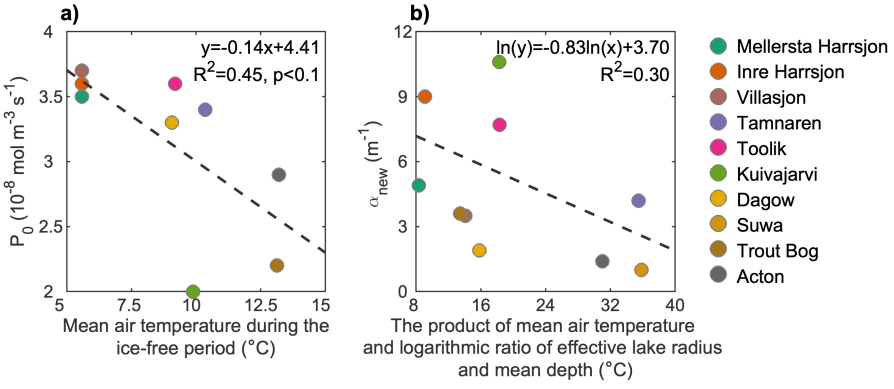

Figure 7: Relationships between CH_4-related model parameters and lake properties. (**a**) Relationship between the CH_4 production rate constant (**P_0**) and mean air temperature during the ice-free period for 9 lakes excluding Lake Suwa. (**b**) Relationship between the constant controlling the decrease in CH_4 production with sediment depth (**α_{new}**) and the product of mean air temperature and the logarithmic ratio of effective lake radius to mean depth (**$lg(\sqrt{lake\ area}/depth/\sqrt{\pi})$**) for 10 lakes. Dashed lines represent the fitted regression.

4.3 Model calibration in tropical deep lakes

We calibrated the model using observations of diffusive CH_4 fluxes from five AGLs, where continuous measurements were conducted over periods ranging from 4 to 66 days (Table 1). Due to the unavailability of observed temperature profiles, we used the satellite-derived lake surface water temperature data from ARC-Lake during the period 1996–2012 to calibrate the light extinction coefficient (Fig. S14 and Table S1 in the Supplement). Considering that the observed flux represents a single value for each of the five AGLs, we calibrated the CH_4-related parameters by initially setting q_{10} to 2.5 and calculating P_0 and α_{new} based on the equations shown in Fig. 7. However, the initial settings of CH_4-related parameters lead to an overestimation of diffusive fluxes. To reduce the simulated fluxes, we found that manually setting α_{new} to 11 m^{-1}, which is the maximum calibrated value among the 10 boreal and temperate lakes (Table S1 in the Supplement), effectively decreased the simulated

https://doi.org/10.5194/egusphere-2026-2349
Preprint. Discussion started: 10 June 2026

fluxes. The RMSE between simulated and observed diffusive CH_4 fluxes across the 5 lakes is 1.5 mg m^{-2} day^{-1} (Fig. 8). This indicates that the calculation of α_{new} is not applicable to the AGLs, leading to an underestimated α_{new} and an overestimation of diffusive CH_4 fluxes. Given that the depths of the five AGLs range from 25 to 572 m, we hypothesized that the overestimation may particularly affect lakes deeper than 25 m, which have lower α_{new} calculated using the equation in Fig. 7b. This overestimation could lead to higher CH_4 emissions in deep lakes compared to shallow lakes, which contradicts previous understanding based on observations (Holgerson and Raymond, 2016). Therefore, we set α_{new} to 11 for all deep lakes (>25 m) in tropical regions, while for other lakes, α_{new} is calculated based on the equation shown in Fig. 7.

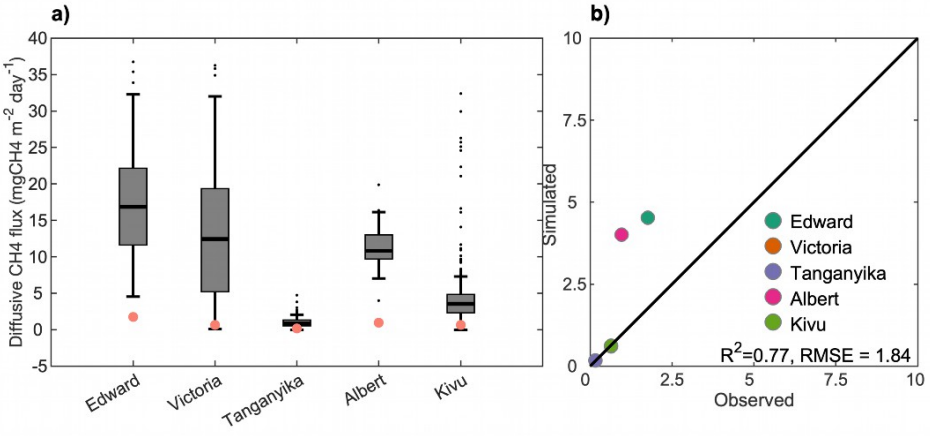

Figure 8: Performance of LAKE2.6 in simulating diffusive fluxes at 5 tropical lakes. (**a**) Boxplots show the distribution of simulated diffusive CH_4 fluxes within a 30-day window for each observation date. The black box encompasses fluxes between the 25th and 75th percentile, with the bold lines indicating the median and black dots outside the box indicating outliers. Red dots indicate the observations. (**b**) Comparison between observed fluxes and the simulated fluxes closest to observations.

5 Model validation

To evaluate the model performance for the CH_4-related parameter set, we first validated the model in 155 boreal and temperate lakes (See Section 3.2) by setting P_0 and α_{new} based on their respective relationships (Fig. 7) and setting q_{10} to 2.5. Considering that α_{new} calculated based on its relationship in 15 lakes (9%) was below the minimum calibrated value (α_{new} = 1 m^{-1}), we set α_{new} to 1 m^{-1} for these lakes (Table S1 in the Supplement). Fig. 9 shows the comparison between the simulated and observed total CH_4 flux, as well as the two pathways of CH_4 flux. Among the 155 lakes, 125 lakes (81%) had observed total CH_4 fluxes < 180 mg CH_4 m^{-2} day^{-1}, which were well captured in the model simulation, with the R^2 between observation and simulation for total flux, diffusive flux and ebullitive flux >0.75. The deviation shows that the model tends to underestimate CH_4 fluxes in boreal and temperate lakes for both diffusion and ebullition, especially in lakes with higher observed fluxes. In contrast, the evident overestimation occurs in four low-latitude reservoirs (around 34–35 °N), where the simulated CH_4 flux exceeds the observed flux by 1.3 to 7 times. For the 30 lakes with observed total CH_4 flux exceeding 180 mg CH_4 m^{-2} day^{-1},

https://doi.org/10.5194/egusphere-2026-2349
Preprint. Discussion started: 10 June 2026

LAKE2.6 was unable to accurately simulate the high CH_4 flux hotspots, especially for the stochastic ebullition. Specifically, the model underestimated the CH_4 flux in 26 lakes, with the simulated flux being 1–96% lower than the observed CH_4 flux.

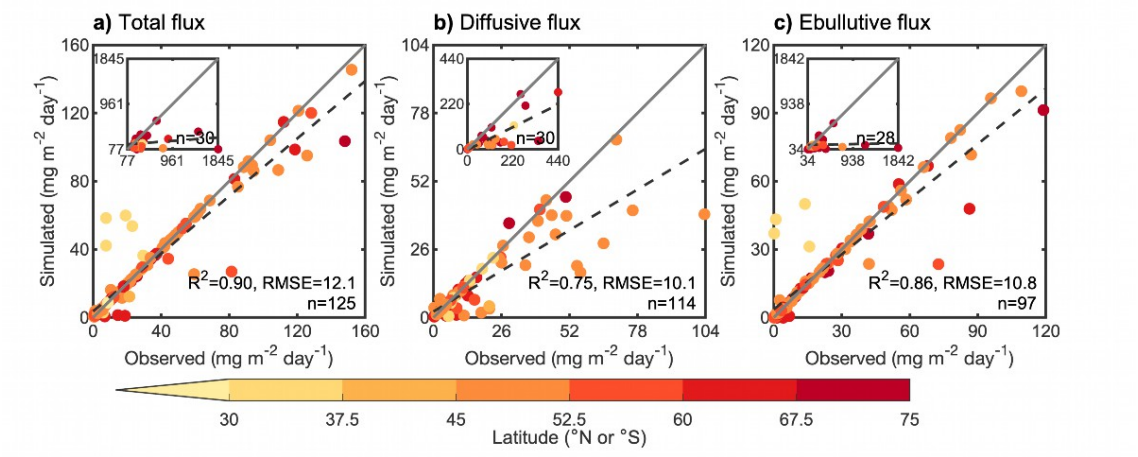

Figure 9: Model validation in 155 boreal and temperate lakes using the CH_4-related parameter set established after model calibration. Panels show the comparison of the total fluxes (**a**), diffusive fluxes (**b**) and ebullitive fluxes (**c**) between simulation and observation for lakes with observed total CH_4 fluxes <120 mg CH_4 m^{-2} day^{-1}. Insets present comparisons for lakes with observed total fluxes >120 mg CH_4 m^{-2} day^{-1}. Note that the number of lakes differs in panels (**b**) and (**c**) because lakes with observed ebullitive fluxes equal to 0 were excluded.

We then validated the model in 21 tropical lakes with observed diffusive CH_4 flux (Fig. 10) applying the same CH_4-related parameter set, and setting α_{new} to 11 m^{-1} for the lake deeper than 25 m. Among the 17 lakes (81%) with observed fluxes < 100 mg CH_4 m^{-2} day^{-1}, the model could capture the magnitude of CH_4 flux in 13 lakes, including the lake deeper than 25 m (Lake Nkugute), where the observed and simulated diffusive flux were 2.6 and 1.4 mg CH_4 m^{-2} day^{-1}, respectively (Fig. 10a). However, the model exhibited overestimation in 12 of 17 lakes, where the simulated diffusive flux exceeds the observed flux (1.4 mg CH_4 m^{-2} day^{-1}) by up to 17 mg CH_4 m^{-2} day^{-1} (Fig. 10b). The overestimates of model could be attributed to the calculated α_{new} ,with all 13 lakes having values under 2.1 m^{-1}, falling at the lower end of calibrated α_{new} range (1–11 m^{-1}) in model calibration. The model underestimated CH_4 flux in the 4 lakes with observed diffusive flux > 100 mgCH_4 m^{-2} day^{-1}, including Lac Vert, Katinda, Kitagata and Nyamunuka (Fig. 10c, d). Similar to boreal and temperate lakes, the high observed flux can be attributed to the methanogenesis resulting from high productivity, which could not be captured in LAKE 2.6.

https://doi.org/10.5194/egusphere-2026-2349
Preprint. Discussion started: 10 June 2026

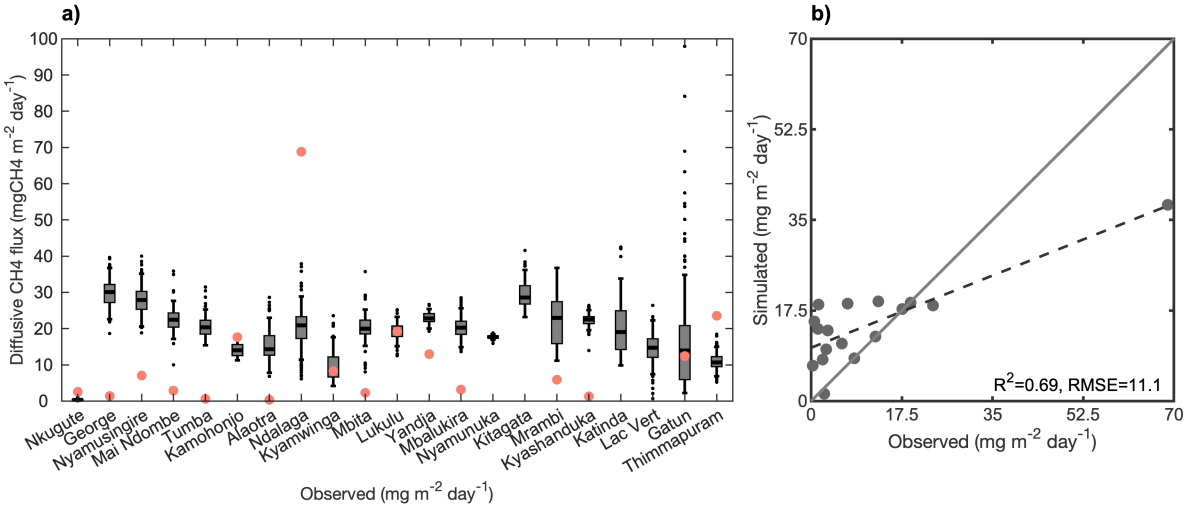

Figure 10: Model validation in 25 tropical lakes under the set of CH_4-related parameterizations established after model calibration. (a) Boxplots show the distribution of simulated diffusive CH_4 fluxes and red circles show the observations. (b) Comparison between observed and simulated diffusive fluxes. Note that lakes with observation > 100 mg CH_4 m^{-2} day^{-1} (Lac Vert, Katinda, Kitagata and Nyamunuka) were excluded in Panel (**b**) and their observations are not shown in Panel (**a**).

6 Global parameterizations and simulations

6.1 Global parameterization framework

Running the LAKE2.6 model individually for 1.4 million water bodies in HydroLAKES is computationally expensive, we developed a global parameterization framework for the simulation setup (Fig. 11). Specifically, lakes in HydroLAKES were aggregated into 2° × 2° grid cells and classified into five depth zones (0–2 m, 2–5 m, 5–10 m, 10–25 m and >25 m) within each grid cell, thereby reducing the number of lakes while emphasizing the role of lake depth in CH_4 emissions (Holgerson and Raymond, 2016). Within each 2° × 2° grid cell, lakes in each depth zone were considered as a single "lake grid cell". As a result, a total of 14,844 lake grid cells were used for model simulation in this study.

For each lake grid cell, we set the light extinction coefficient following Håkanson (1995), q_{10} to 2.5, and P_0 based on the relationship established with the mean air temperature during the ice-free months of the corresponding 2° × 2° grid (Fig. 12). The α_{new} for lake grid cells deeper than 25 m between 30 °N and 30 °S was set to 11, while for others, it is calculated using the relationships based on the mean air temperature and lake morphometric properties of each lake grid cell (Fig. 12). Based on the model calibration results for α_{new}, we hypothesized that the range of α_{new} should be limited to 1–11 to ignore the extrapolation problem, which alters the calculated α_{new} values in 5.8% of the lake grid cells. For the other parameters, including Δt, M, ns and spinup period, their settings in LAKE2.6 are consistent with those used for model calibration and validation in lakes (See Section 3.2). The depth and area of each lake grid cell were represented by the median lake depth and the logarithmic mean lake area, respectively. The total CH_4 emissions for each lake grid cell at each time step were then

https://doi.org/10.5194/egusphere-2026-2349
Preprint. Discussion started: 10 June 2026

calculated by multiplying the simulated CH_4 flux from the global parameterization framework by the total lake area within lake grid cell.

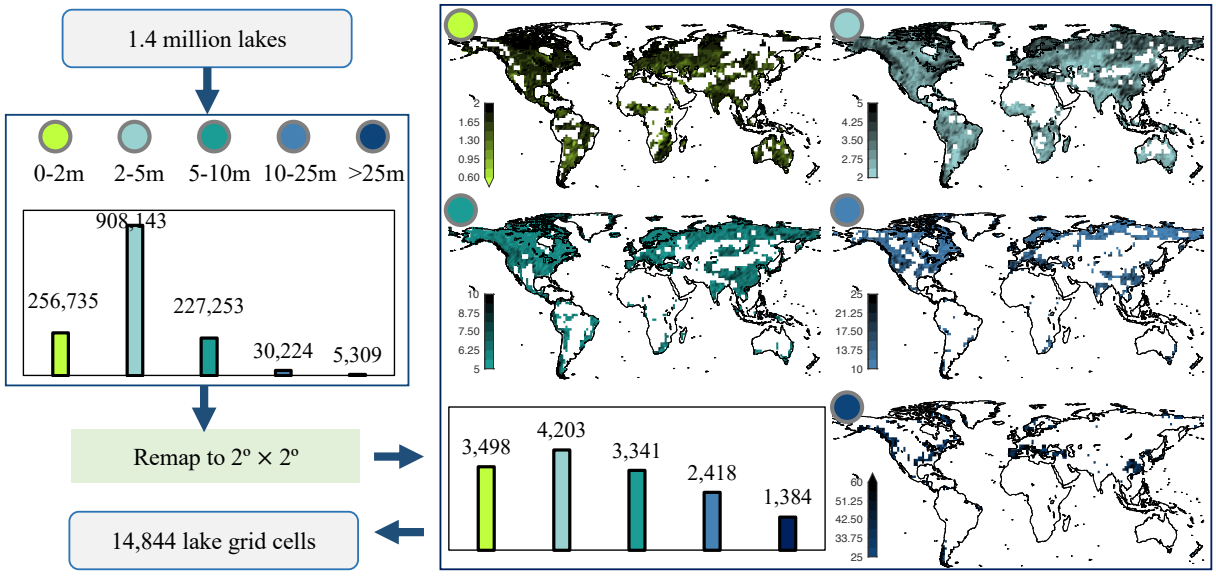

Figure 11: Schematic diagram of the global parameterization framework for LAKE2.6.

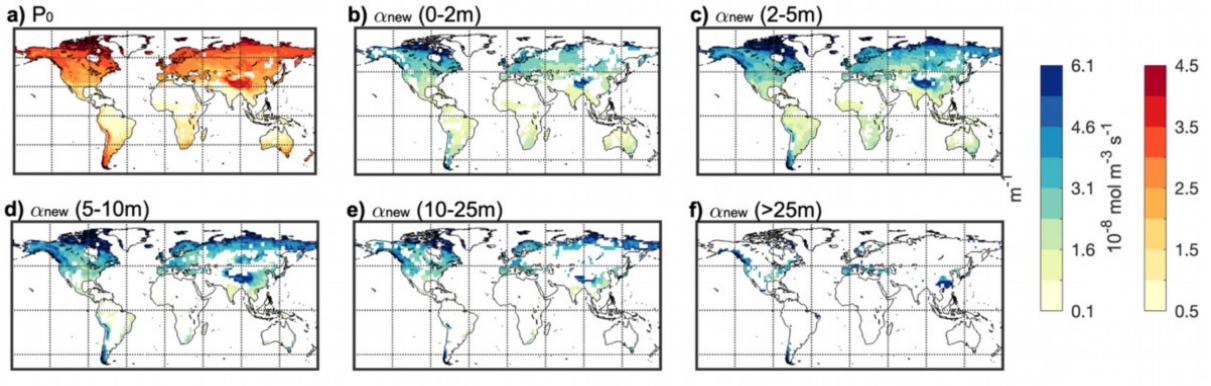

Figure 12: Spatial pattern of the CH_4-related parameters, including $\mathbf{P_0}$ (**a**) and $\boldsymbol{\alpha_{new}}$ across 5 depth zones: 0–2 m (**b**), 2–5 m (**c**), 5–10 m (**d**), 10–25 m (**e**) and >25 m (**f**).

6.2 Global simulation of lake CH_4 emissions

Based on the global parameterization framework, we conducted a global simulation across 14,844 lake grid cells during the period from 1979 to 2023. The simulated global lake CH_4 emissions range from 17.7 to 20.1 Tg CH_4 yr^{-1} over the period, with ebullition accounting for 78–80% (14.1–16.0 Tg CH_4 yr^{-1}) and diffusion accounting for 20–22% (3.5–4.2 Tg CH_4 yr^{-1}) of the total annual CH_4 emissions. Compared to recent estimates, our results are consistent in magnitude but slightly lower than the

https://doi.org/10.5194/egusphere-2026-2349
Preprint. Discussion started: 10 June 2026

model estimates from Zhuang et al. (2023) which reported 24.0 ± 8.4 Tg CH_4 yr^{-1} for the period 2004–2006. The discrepancy in estimates lies in the lack of consideration of permafrost-affected lake in this study, which led to higher CH_4 emission estimate for the sub-arctic region (>50 °N) in Zhuang et al. (2023) (7.4 Tg CH_4 yr^{-1}), compared to 3.8–5.2 Tg CH_4 yr^{-1} in our study. The dominance of ebullition is consistent with results both from recent model simulation and data-driven approaches, with the ratio of ebullition falling within ranges estimated in these studies (56–89%) (Johnson et al., 2022; Zhuang et al., 2023) . In tropical area, our estimates for diffusion and ebullition are 1.4–1.5 and 5.7–6.4 Tg CH_4 yr^{-1}, respectively, aligning with the data-driven estimates of Borge et al., which reported results of 1.6 ± 0.4 and 1.7–11.4 Tg CH_4 yr^{-1} for diffusion and ebullition, respectively (Borges et al., 2022). Excluding the 6,687 reservoirs in HydroLAKES (which cover 9% of the total area), simulated lake CH_4 emissions range from 15.3 to 17.5 Tg CH_4 yr-1, which falls within the ranges of recent estimates from global CH_4 budget (13–53 Tg CH_4 yr^{-1}) (Saunois et al., 2025). The mean annual total CH_4 flux for the period 1980–2023 is 7.6 mg CH_4 m^{-2} day^{-1}, with 1.6 mgCH_4 m^{-2} day^{-1} for diffusion and 6.0 mg CH_4 m^{-2} day^{-1} for ebullition, respectively. The model results show a latitudinal pattern in CH_4 flux, with values of 3.6, 8.6 and 18.1 mg CH_4 m^{-2} day^{-1} for the sub-arctic, temperate and tropical regions, respectively (Fig. 13), which is consistent with the results from Zhuang et al. (2023). Given the lack of inter-annual simulations of global lake CH_4 flux in other studies, our results provide a reliable estimate using LAKE2.6 based on the global parametrization scheme, with a detailed analysis to be presented in future studies.

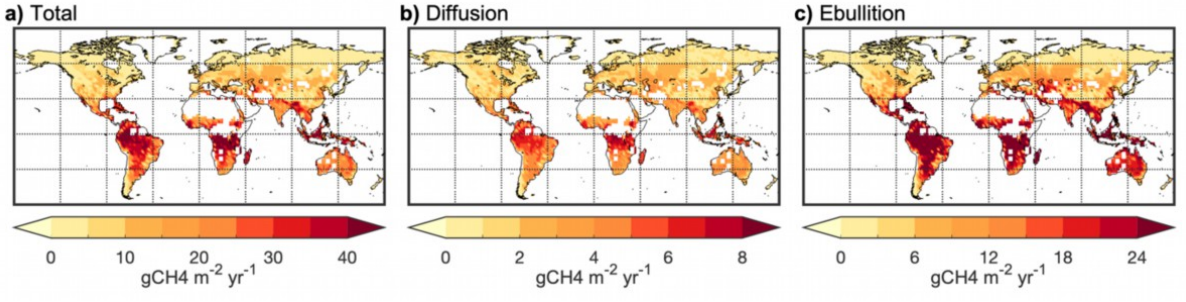

Figure 13: Spatial pattern of mean annual total CH_4 flux (**a**), diffusive flux (**b**) and ebullitive flux (**c**) during the period 1980–2023.

7 Discussion

7.1 Improvements of simulation using LAKE2.6

The LAKE2.6 model relates CH_4-related processes to substrate requirements and environmental factors through several empirical parameters. The original model was applied for CH_4 simulation at site-level calibration, by tuning different empirical parameters (Stepanenko et al., 2011; Walter and Heimann, 2000; Guseva et al., 2016; Stepanenko et al., 2016). After conducting Sobol sensitivity analysis on 15 parameters related to CH_4 process in LAKE2.6, we tuned only the three most sensitive parameters and obtained comparable results across 15 lakes in this study, which contributed to applying the process-based model from site-level calibration to global-level simulation. We found that parameters representing the quantity and quality of substrates for methanogenesis are more sensitive than other parameters (Table 1), implying that anoxic CH_4

https://doi.org/10.5194/egusphere-2026-2349
Preprint. Discussion started: 10 June 2026

production rate is a key determinant of CH_4 flux (Bertolet et al., 2020). By tuning parameters related to CH_4 production, including P_0, α_{new} and q_{10}, the LAKE2.6 performs well in simulating continuous monthly and annual CH_4 fluxes at 10 boreal and temperate lake sites (Figs. 4–6), as well as simulating the mean flux averaged over several consecutive days at 5 tropical lakes (Fig. 8). Besides, the tuned parameters are comparable in magnitude to those from previous model calibrations, with P_0, α_{new} and q_{10} tuned in the ranges of 3×10^{-8}–4×10^{-8} mol m^{-3} s^{-1}, 3–5 m^{-1}, and 2–6, respectively, in previous site-level model calibration studies using the LAKE model. The good performance of the model at the 15 lake sites with site-specific tuned parameters demonstrates that using LAKE2.6 is reliable for simulating CH_4 emissions from tropical to sub-arctic lakes, as the mean depth and surface area ranges of the 15 lakes account for 89% of the global number of lakes and 40% of total area in HydroLAKES.

In contrast to previous model studies using a region-specific parameterization for global-scale simulation, we developed a CH_4-related parameterization scheme by linking two sensitive parameters (P_0 and α_{new}) to lake-specific properties based on site-level model calibrations (Fig. 7). The established relationships for P_0 and α_{new} are consistent with observed variations in the quantity and quality of organic carbon in lake sediments which reflect the potential for methanogenesis across different lakes. Specifically, we related P_0, which represents the quantity of sediment organic carbon, to the mean air temperature during the ice-free months of each lake (Fig. 7a). As warmer lakes lead to greater mineralization and thus less remainder of organic carbon (Gudasz et al., 2010), the relationship of P_0 suggests that lakes in colder climates tend to provide more labile carbon for CH_4 production than warmer lakes. For α_{new} which reflects the relative vertical distribution of organic carbon by controlling its rates of decline with sediment depth, a higher α_{new} indicates a more heterogenous vertical profile, while a lower α_{new} indicates a more homogeneous vertical distribution shown in Eq. (A2) in Appendix A. Considering that enhanced mineralization in warmer climates primarily occurs in surface sediments (Håkanson, 1982), the reduced amount of organic carbon in warmer lakes could result in a more homogeneous vertical distribution of organic carbon. Consequently, these lakes are likely to have lower α_{new} than colder lakes (Fig. 7b). Besides, as one of the important lake morphological factors, the dynamic ratio ($\sqrt{lake\ area}/depth$) reflects lake energy and slope, which determines the ratio of lake sediment transportation area rather than the accumulation area to lake bottom area (Håkanson, 1982). Lakes with higher dynamic ratios are considered to be dominated by erosion and transportation processes driven by resuspension rather than accumulation (Håkanson, 1982). These lakes exhibit a more homogeneous vertical distribution of organic carbon (Ostrovsky and Tęgowski, 2010), and thus tend to have lower α_{new} than lakes with lower dynamic ratios (Fig. 7b).

Compared with previous data-driven studies, global simulation results from LAKE2.6 could explicitly show the spatial and temporal variability of CH_4 fluxes by applying a CH_4-related parameterization scheme and incorporating seasonal variation through a process-based approach. Additionally, the global lake modelling framework developed in this study enables long-term simulations of lake CH_4 emissions at the global scale using a process-based model (Fig. 13). By dividing lakes into 5

https://doi.org/10.5194/egusphere-2026-2349
Preprint. Discussion started: 10 June 2026

depth zones and subsequently aggregating lakes within each depth zone of 2° × 2° grid into a single "lake grid cell", this framework not only reduces computational costs, but also accounts for the role of lake depth on determining the magnitude of CH_4 flux (Deemer and Holgerson, 2021). For example, our results show that simulated annual total CH_4 fluxes decrease significantly with increasing lake depth zones (Fig. S15 in the Supplement; $p < 0.01$), with the highest CH_4 flux in lakes with depth of 0–2 m (20.0 mg CH_4 m^{-2} day^{-1}) and lowest in lakes deeper than 25 m (0.3 mg CH_4 m^{-2} day^{-1}). Although lakes shallower than 5 m account for only 1% of the global lake area, they contribute over 63% of the total annual CH_4 emissions, highlighting the disproportionate role of small lakes in global lake CH_4 emissions (Rosentreter et al., 2021). As a result, the long-term simulation results provide a foundation for future attribution of global lake CH_4 emissions at both global-level and regional-level scale.

7.2 Comparison of simulation and observation of CH_4 fluxes

In this study, the global implementation of LAKE2.6 is based on its good performance in reproducing the magnitude of observed CH_4 fluxes. However, noticeable biases remain between the simulated and observed CH_4 fluxes from monthly to annual scales (Figs. 4–6), which affect the accuracy of reproducing the seasonal cycle of lake CH_4 emissions (Fig. S16 in the supplement). As LAKE2.6 is forced by climate variables with fixed parameters, the biases may reflect the lack and/or the uncertainties of temporal variation in simulated processes that regulate the rate of CH_4 production, oxidation and transport. Previous studies showed that lake productivity strongly influences CH_4 fluxes across lakes, as higher nutrients input enhance phytoplankton metabolic activity and increase the supply of substrates for sediment methanogenesis (Beaulieu et al., 2019). Among other things, LAKE2.6 constrains CH_4 production rates only using climatological data and lake properties, without considering the quantity of substrates from biological activity and organic carbon inputs, which are closely related to the trophic state of lakes (Suresh et al., 2023). The lake trophic state in LAKE2.6 is determined by the light extinction coefficient, which controls the vertical distribution of light and is further used to estimate the oxygen concentration in the photic zone, defined as the depth where light intensity > 1% of surface radiation. In other words, the model lacks parameterization of lake productivity, as it relies on a fixed light extinction coefficient that is independent of substrates for methanogenesis. For lakes with abundant substrates and complex carbon sources, the model may further underestimate the magnitude of CH_4 fluxes. This could explain the noticeable bias for 26 boreal and temperate lakes with total CH_4 fluxes exceeding 180 mg CH_4 m^{-2} day^{-1} during model validation (Fig. 9). Among the 26 lakes, 22 are surrounded by permafrost, peaty substrates, or urban areas, are dominated by agricultural land use and are classified as metro-eutrophic or eutrophic lakes (Erkkila et al., 2018; Palma-Silva et al., 2013; Van Bergen et al., 2019). In light of this, our estimate of global lake CH_4 emissions is conservative, as it underestimates lake turbidity and does not account for dynamic trophic states, leading to inaccuracies in quantifying CH_4 production rates for each lake grid cell.

The calibrated light extinction coefficient is convincing for 6 calibrated lakes with observed temperature profiles (Table 1), which show good agreement with the simulations (Figs. S8-13 in the Supplement) and serve as proxies for lake thermal

https://doi.org/10.5194/egusphere-2026-2349
Preprint. Discussion started: 10 June 2026

dynamics (Woolway et al., 2021). Considering the observed temperature profile gaps in the other 7 calibrated and all validated lakes, the light extinction coefficient calculated using an empirical equation or calibrated based on lake surface temperature might introduce uncertainties in thermal dynamics, which further influence CH_4 transport processes and bias the simulated CH_4 fluxes (Mendoza-Pascual et al., 2021). Mechanistically, the 1-D model cannot realistically simulate thermal dynamics because it uses mean or maximum depth to represent the complex 3D lake bathymetry, which is a key factor influencing thermal dynamics (Mendoza-Pascual et al., 2021). This bias could be more evident in lakes with higher dynamic ratio affected by horizontal mixing. Such processes are not represented in 1-D models, which instead assume horizontally averaged conditions across the lake. Additionally, the parameterizations of wind mixing and turbulent mixing in the 1-D model introduce considerable uncertainty in simulating lake thermal dynamics, including effects on the temporal variation of lake temperature profiles as well as the timing of stratification onset and breakdown (Woolway et al., 2021). Although it is difficult to quantify these uncertainties due to the lack of continuous observations, previous studies based on limited CH_4 flux measurements often focus on the spring overturn period following ice breakup, during which fluxes account for 4–74% of the annual CH_4 emissions (Jansen et al., 2019). Spring CH_4 emissions in ice-covered lakes occur during the overturn period after ice breakup, when the CH_4 that accumulated under the ice is released as hypolimnetic water mixes with the epilimnion (Jammet et al., 2015). While LAKE2.6 releases the accumulated CH_4 immediately after ice breakup, the model may shift the timing of CH_4 emissions earlier than observed (Fig. S16 in the Supplement). Nevertheless, this bias may be negligible at the monthly scale. For 7 of the 15 calibrated lakes that experience ice cover for more than 3 months, CH_4 emissions during the ice-off month account for 13–57% of the annual total, which falls within the range reported in previous study (Jansen et al., 2019).

In addition to model limitations, measurement uncertainties may also bias lake CH_4 flux estimates, including those associated with widely used floating chambers, bubble traps, and EC methods. The continuously observed CH_4 fluxes in this study represent only limited lake areas, as measurements were obtained from 17–21 point-based instruments (including bubble traps and floating chambers) or from a single EC tower. The continuously observed CH4 fluxes in this study represent only limited lake areas, as each lake was equipped with 17–21 point measurement devices (including bubble traps and floating chambers) or a single EC tower. Due to the spatial variations in CH_4 fluxes associated with lake depth, with higher fluxes near the shore and lower in the middle of the lake, observations may underestimate or overestimate whole-lake CH_4 flux, depending on the deployment places of devices and footprints of the EC tower (Nemitz et al., 2018). For Lake MH, IH and VS, CH_4 ebullition measurements using bubble traps might omit the sporadic CH_4 ebullitive events (Jammet et al., 2017). Moreover, partitioned CH_4 fluxes from Lake VS and the adjacent fen exhibit distinct seasonal patterns, with peak emissions occurring during the spring overturn in the lake, whereas in the fen, peaks occur in summer (Jammet et al., 2017). Considering the hydrological connections between lakes and surrounding ecosystems, the observations could include CH_4 fluxes from more than one ecosystem, with similar magnitude but different seasonal cycles compared to those from the lake. Such uncertainties are particularly critical for lakes used in model validation, where observation gaps in both time and space further limit the accuracy of comparison.

https://doi.org/10.5194/egusphere-2026-2349
Preprint. Discussion started: 10 June 2026

7.3 Future directions of LAKE development and application

Based on model calibration and validation in more than 191 lakes around the world, LAKE2.6 could be applied to analyse lake biogeochemical processes at both regional and global scales. In regions with limited observations, particularly in tropical areas, the model enables prediction of lake CH_4 emissions based on climate forcing and lake characteristics. With more regions providing continuous observations in the future, a more robust parameterization in CH_4-related parameters could be established through model calibration and validation. Moreover, the global implementation of LAKE2.6 in this study made it possible to conduct multi-year simulations of global lakes. Given that climate has changed lake physical processes (Woolway et al., 2020), LAKE2.6 could be used to quantify the further effects of climate change on lake CH_4 emissions through process-based simulations and to conduct future projections under different climate scenarios. With more global data on lake morphometric characteristics becoming available, besides, the model could provide initial predictions of the influence of dynamic lake area on CH_4 emissions (Li et al., 2025). Future improvements in computational efficiency could allow the use of more depth zones, particularly to better represent shallow lakes, while still reducing overall computational costs. Moreover, future computational efficiency facilitates model incorporation into larger frameworks, such as regional climate models or Earth system models.

The simulated CH_4 fluxes from LAKE2.6 are attributed only to abiotic factors, including lake properties and climate variables, without explicitly considering biological processes such as phytoplankton metabolic activities, which can be enhanced by nutrient inputs from the catchment. Future development of more advanced lake models is required to better parameterize the aforementioned biological and physical processes. Some of these processes have been partially included in existing biogeochemical 1-D lake models, such as ALBM and FLAME (Maisonnier et al., 2025; Tan et al., 2024). Nevertheless, due to limited observations and incomplete understanding of the underlying mechanisms of lake eutrophication, incorporating these processes still introduces significant uncertainties in global estimates, especially given the poor constraints from observed CH_4 fluxes in lakes worldwide. As turbid lakes can be eutrophic, humic, or rich in colored dissolved organic carbon (DOC), the relationship between the light extinction coefficient and trophic state in LAKE2.6 may lead to an overestimation of trophic status in humic or highly colored lakes, and an underestimation in genuinely eutrophic systems. Considering that machine learning models have been used to address the limited dataset size, future directions could focus on developing hybrid models to better represent uncertain biological processes, including lake trophic state and light extinction coefficients.

8 Conclusions

So far global lake CH_4 emission estimates have mostly used data-driven or meta-analysis approaches, which causes the large uncertainties. In this study, we used a one-dimensional process-based model LAKE2.6 to simulate lake CH_4 emissions from site level to the global scale. Instead of using region-specific parameters, we developed a site-specific parameterization scheme by tuning the most sensitive CH_4-related parameters and linking them to lake properties. Furthermore, we established a global parameterization framework to reduce the number of modelled lakes required for global CH_4 simulations while emphasizing

https://doi.org/10.5194/egusphere-2026-2349
Preprint. Discussion started: 10 June 2026

the role of lake depth in CH_4 emissions. Using this framework, we estimated that global lakes emitted 17.7–20.1 Tg CH_4 yr^{-1} during 1979–2023. This estimate falls within the range of recent global CH_4 budget assessments with a clear latitudinal pattern in CH_4 flux. The explicit spatial and temporal variability captured by LAKE2.6 provides a foundation for future detecting and attribution of long-term changes in global lake CH_4 emissions under a warming climate.

Appendix A: The CH_4-related equations in LAKE2.6

The biogeochemical module in LAKE2.6 is based on the model developed by Walter et al., which is one of the most widely used models for global wetland CH_4 simulation (Walter and Heimann, 2000). The CH_4 concentration in sediment column ($C_{CH_4,s}$) at each time step (t) varies vertically with the CH_4 production, oxidation and transport, expressed as the following equation:

$$\frac{\partial C_{CH_4,s}}{\partial t} = \frac{\partial}{\partial z_s} k_{CH_4,s} \frac{\partial C_{CH_4,s}}{\partial z_s} + P_{CH_4,s} - E_{CH_4,s} - O_{CH_4,s}, \quad \text{(A1)}$$

Where $k_{CH_4,s}$ is the diffusion coefficient of sediment dissolved CH_4, z_s is the vertical coordinate directed downward from the sediment surface, and $P_{CH_4,s}$, $E_{CH_4,s}$ and $O_{CH_4,s}$ are CH_4 production rates, CH_4 ebullition rates, and CH_4 oxidation rates in the sediment column, respectively. Sediment CH_4 is produced both in the top sediment layers from newly degraded organic matter and in the bottom layers from organic-rich sediments, primarily in thermokarst lakes formed by the collapse of permafrost soils. In this study, we only consider CH_4 production in top sediment layers, and the CH_4 production rate is calculated as follows:

$$P_{new} = P_0 \exp(-\alpha_{new} z_s) H(T - T_{mp}) q_{10}^{\frac{T}{10}} (1 + \alpha_{O_2,inhib} C_{O_2,s})^{-1}, \quad \text{(A2)}$$

Where P_0 is the CH_4 production rate constant representing the quantity and quality of organic matters. α_{new} is a constant set to 3 m^{-1} that controls the magnitude of decrease in CH_4 production rate with increasing z_s. $H(T - T_{mp})$ is the Heaviside function of temperature T and T_{mp} is the melting point temperature. q_{10} is the temperature dependence factor to T and set to 2.3. $\alpha_{O_2,inhib}$ is a constant of 316.8 m^3 mol^{-1}, indicating that CH_4 production rate decrease to 1% when the O_2 concentration in sediment columns ($C_{O_2,s}$) exceeds 10 ppm ($Conc_{O_2,inhib}$). Likewise, the concentration of SO_4^{2-} suppresses CH4 production rate to zero when it exceeds 30 μmol L^{-1} ($Conc_{SO_4,inhib}$), which is not explicitly shown in Eq. (A2). Both the concentrations of O_2 and SO_4^{2-} decrease exponentially with the coordinate z_s in sediment columns, at the rate of 6.6 ($Decay_{O_2,exp}$ and $Decay_{SO_4,exp}$). P_{new} can increase the change in $C_{CH_4,s}$, as shown in equation Eq. (A1). When the gas phase of $C_{CH_4,s}$ exceeds the critical value, the process of ebullition can occur immediately in the model, calculated as follow:

$$E_{CH_4,s} = \max\{0, c_e[C_{CH_4,s} - \alpha_e C_{CH_4,cr}(p_a, h, C_{N_2}, \Pi)]\}, \quad \text{(A3)}$$

Where c_e is the rate constant set to 2.78×10^{-4} s^{-1}, α_e is relative constant for critical CH_4 concentration and set to 0.4. $C_{CH_4,cr}$ represents the maximum CH_4 concentration in the sediment under given temperature and pressure (p_a) and porosity (Π) at

https://doi.org/10.5194/egusphere-2026-2349
Preprint. Discussion started: 10 June 2026

depth h, assuming that only CH_4 and N_2 exist. $E_{CH_4,s}$, along with N_2, O_2, CO_2 and Ar, is included in the bubbles with a radius of 2 mm rising from sediment by buoyancy and turbulence. The remaining $C_{CH_4,s}$ is stored in the sediment column as a dissolved phase, with the dissolved $C_{CH_4,s}$ in layers <1 cm assumed to be oxidized by biological processes (Liikanen et al., 2002). Michaelis–Menten equation is used to calculate sediment CH_4 oxidation rate in the model, expressed as follow:

$$O_{CH_4,s} = V_{max,s} \frac{C_{CH_4,s}}{K_{CH_4,s}+C_{CH_4,s}} \frac{C_{O_2,s}}{K_{O_2,s}+C_{O_2,s}}, \quad \text{(A4)}$$

Where $V_{max,s}$ is the potential oxidation rate set to 1.11×10^{-5} mol m^{-3} s^{-1}, $K_{CH_4,s}$ and $K_{O_2,s}$ are half-saturation constants of CH_4 and O_2 for sediment oxidation, with the value of 9.5×10^{-3} and 2.1×10^{-2} mol m^{-3}, respectively. Other process of sediment CH_4 oxidation is also considered in the model by multiplying the Sedimentary oxygen demand (SOD) by a factor (methox2sod), which is set to zero in the model.

CH_4 concentration (C_{CH_4}) in the water column varies with the water level, CH_4 diffusive processes and other sources and sinks, expressed below:

$$\frac{\partial C_{CH_4}}{\partial t} = \frac{B_s}{h}\frac{\partial C_{CH_4}}{\partial \xi} + \frac{1}{Ah^2}\frac{\partial}{\partial \xi}\left(Ak_s \frac{\partial C_{CH_4}}{d\xi}\right) + B_{CH_4} - O_{CH_4}, \quad \text{(A5)}$$

Where B_s/h represents the change in water level with B_s representing water budget defined as precipitation minus evaporation. k_s is the diffusion coefficient of dissolved CH_4, set to same value of $k_{CH_4,s}$. B_{CH_4} represents dissolved CH_4 from bubble dissolution due to the change in bubble radius during transport. O_{CH_4} represents the CH_4 oxidation rate in the water column, calculated using Michaelis–Menten equation (Eq. 4). The potential oxidation velocity ($V_{max,w}$) is set to 1.16×10^{-5} mol m^{-3} s^{-1} and half-saturation constants of CH_4 ($K_{CH_4,w}$)and O_2 ($K_{O_2,w}$) for water column set to 3.75×10^{-2} mol m^{-3} and 2.1×10^{-2} mol m^{-3}, respectively.

Two pathways of CH_4 emission are considered in the model: ebullition and diffusion. Ebullitive flux originates from bubble dissolved at the surface, emitted immediately during the open-water period and accumulated during the ice-cover period. In the model, only 90% (denoted as $Intercept_{bubble}$) of bubble CH_4 accumulates under water surface and 67.5% (denoted as $Decrease_{CH_4,w}$) of the accumulated CH_4 is emitted once the ice breaks up, while the remained 37.5% of CH_4 is oxidized. The diffusive flux in the model is calculated by the following equation:

$$F_{C_w} = K_{ge}(C_w|_{z=0} - C_{ae}), \quad \text{(A6)}$$

Where K_{ge} is the piston velocity indicating the rate of gas exchange. $C_w|_{z=0}$ is the dissolved CH_4 concentration at the lake surface and C_{ae} is the equilibrium dissolved CH_4 concentration relative to atmospheric CH_4, calculated by Henry Law. The surface renewal model (Heiskanen et al., 2014) is used to calculate K_{ge} in the model as follow:

$$K_{ge} = \frac{C_{1,SR}(\epsilon|_{z=0}\upsilon_m)^{1/4}}{\sqrt{Sc(T)}}, \quad \text{(A7)}$$

https://doi.org/10.5194/egusphere-2026-2349
Preprint. Discussion started: 10 June 2026

Where $C_{1,SR}$ is the empirical constant set to 0.5, $\epsilon|_{z=0}$ is surface kinetic energy dissipation calculated in hydrodynamic module of the model, $Sc(T)$ is the Schmidt number based on temperature T and υ_m is the molecular diffusion coefficient, set to 1.31×10^{-6} m^2 s^{-1}.

Appendix B: List of major parameters in CH_4-related equations of the LAKE 2.6 model

Process	Parameter	Definition	Initial values	Ref.
CH_4 production	q_{10}	a constant controlling the rate of CH_4 production in sediments with a 10 °C rise in temperature	2.3	Liikanen et al. (2002)
	P_0	CH_4 production rate constant in sediments (mol m^{-3} s^{-1})	3×10^{-8}	Stepanenko et al. (2016)
	α_{new}	a constant controlling the rate of decrease in CH_4 production with depth in sediments (m^{-1})	3	Beljaars and Holtslag (1991)
	$Conc_{O_2,inhib}$	the concentration of dissolved O_2 inhibiting CH_4 production in sediment (ppm)	10	Borrel et al. (2011)
	$Decay_{O_2,exp}$	the decay rate of O_2 concentration following an exponential law	6.6	-
	$Conc_{SO_4,inhib}$	the concentration of Dissolved SO4 inhibiting CH_4 production in sediment (mmol L^{-1})	30	Lovley and Klug (1986)
	$Decay_{SO_4,exp}$	the decay rate of SO_4^{2-} concentration following an exponential law	6.6	-
CH_4 oxidation	methox2sod	the fraction of sedimentary oxygen demand used for CH_4 oxidation in the top of bottom sediment (%)	0	Liikanen et al. (2002)
	$K_{CH_4,w}$	half-saturation constant for CH_4 during CH_4 oxidation in water (mol m^{-3})	0.0375	Liikanen et al. (2002)
	$K_{O_2,w}$	half-saturation constant for O_2 during CH4 oxidation in water (mol m^{-3})	0.021	Liikanen et al. (2002)
	$V_{max,w}$	CH_4 oxidation potential in oxygen-saturated water (mol m^{-3} s^{-1})	1.16×10^{-5}	Liikanen et al. (2002)
CH_4 transport	c_e	the rate constant of bubble formation (s^{-1})	2.78×10^{-4}	-
	α_e	relative level of the threshold CH_4 concentration for bubble formation	0.4	Tan et al. (2015)

https://doi.org/10.5194/egusphere-2026-2349
Preprint. Discussion started: 10 June 2026

$Intercept_{bubbl}$	The fraction of CH_4 bubbles trapped by the ice cover during a wintertime (%)	90	Stepanenko et al. (2011)
$Decrease_{CH_4,w}$	the fraction of CH_4 remaining in bubble when they have been trapped by the ice cover (%)	62.5	Stepanenko et al. (2011)

Code and data availability

The LAKE2.6 model is open source and available at https://mathmod.org/lake/ (last access: 1 June 2026) with the user guide. The model code used in this study, lake properties for the 15 lakes used for model calibration and the 176 lakes for model validation, as well as all scripts for data processing, model calibration and model validation and global simulation analysis, are available online at https://doi.org/10.5281/zenodo.20482428 (Li, 2026).

Observed ebullitive and diffusive fluxes for MH, IH and VS are available at https://doi.org/10.17043/stordalen-lakes-ch4-ebul-4 (Jansen et al., 2021) and https://doi.org/10.17043/stordalen-lakes-ch4-diff (Jansen et al., 2020a), respectively. Observed total CH_4 fluxes for Lake Acton and Trout Bog are available at https://doi.org/10.17190/AMF/1846660 (Waldo, 2022) and https://doi.org/10.17190/AMF/1804493 (Stoy et al., 2025), respectively. Observed total CH_4 fluxes for Lake Dagow and Lake Suwa are available at https://doi.org/10.18140/FLX/1669633 (Sachs et al., 2018) and https://doi.org/10.18140/FLX/1669648 (Iwata, 2016), respectively. Observed total CH_4 fluxes for Lake Tämnaren, Lake Toolik and Lake Kuivajärvi are available at https://doi.org/10.6073/pasta/87a35ca843d8739d75882520c724e99e (Golub et al., 2022a). Observed temperature profile data for MH, IH and VS lakes are available at https://doi.org/10.17043/stordalen-lake-temperatures-4 (Crill et al., 2021). Temperature profile data for Trout Bog and Lake Acton are available at https://doi.org/10.6073/pasta/9535bbc321ebd512cd0e8b0f1d7821be (Magnuson et al., 2023) and https://doi.org/10.6073/pasta/14a201367db1429e8acbeb7e5a7341b8 (Lottig et al., 2021), respectively.

Lake surface water temperature from ARC-Lake is obtained from http://www.laketemp.net/home_ARCLake/data_access.php. Climate forcing data from ERA5 product is obtained from https://doi.org/10.24381/cds.adbb2d47 (Hersbach et al., 2023). Global atmospheric CO_2 and CH_4 concentrations were obtained from https://doi.org/10.15138/9N0H-ZH07 (Lan et al., 2026) and https://doi.org/10.15138/P8XG-AA10 (Lan et al., 2022), respectively. The HydroLAKES database is available at https://www.hydrosheds.org/products/hydrolakes#downloads and is described in Messager et al. (2016).

https://doi.org/10.5194/egusphere-2026-2349
Preprint. Discussion started: 10 June 2026

Author contribution

S.P designed the project, X.L. conducted the model simulations, performed the analysis and drafted the manuscript. V.S. developed the LAKE model. All co-authors commented and revised the manuscript.

Competing interests

The authors declare that they have no conflict of interest.

Acknowledgements

The authors wish to thank all scientists who have contributed lake methane fluxes observations available for our model calibration and validation, and thank the LAKE model group for their kind help with the model code.

Financial support

This study was supported by the Yunnan Provincial Science and Technology Project at Southwest United Graduate School (grant no. 202302AP370001) and China Postdoctoral Science Foundation (grant no. 2025T180088).

References

Bastviken, D., Cole, J., Pace, M., and Tranvik, L.: Methane emissions from lakes: Dependence of lake characteristics, two regional assessments, and a global estimate, Glob. Biogeochem. Cycles, 18, 10.1029/2004GB002238, 2004.

Bastviken, D., Tranvik, L. J., Downing, J. A., Crill, P. M., and Enrich-Prast, A.: Freshwater methane emissions offset the continental carbon sink, Science, 331, 50, 10.1126/science.1196808, 2011.

Beaulieu, J., DelSontro, T., and Downing, J.: Eutrophication will increase methane emissions from lakes and impoundments during the 21st century, Nat. Commun., 10, 1375, 2019.

Beljaars, A. C. M. and Holtslag, A. A. M.: Flux parameterization over land surfaces for atmospheric models, J. Appl. Meteorol., 30, 327-341, 10.1175/1520-0450(1991)030<0327:FPOLSF>2.0.CO;2, 1991.

Bertolet, B., Olson, C., Szydlowski, D., Solomon, C., and Jones, S.: Methane and primary productivity in lakes: Divergence of temporal and spatial relationships, J. Geophys. Res. Biogeosci., 125, e2020JG005864, 2020.

Borges, A. V., Deirmendjian, L., Bouillon, S., Okello, W., Lambert, T., Roland, F. A. E., Razanamahandry, V. F., Voarintsoa, N. R. G., Darchambeau, F., Kimirei, I. A., Descy, J. P., Allen, G. H., and Morana, C.: Greenhouse gas emissions from African lakes are no longer a blind spot, Sci. Adv., 8, eabi8716, 10.1126/sciadv.abi8716, 2022.

Borrel, G., Jezequel, D., Biderre-Petit, C., Morel-Desrosiers, N., Morel, J. P., Peyret, P., Fonty, G., and Lehours, A. C.: Production and consumption of methane in freshwater lake ecosystems, Res. Microbiol., 162, 832-847, 10.1016/j.resmic.2011.06.004, 2011.

Casper, S. J.: Lake Stechlin: A temperate oligotrophic lake, Springer Science & Business Media2012.

Chechin, D. G., Repina, I. A., and Stepanenko, V. M.: Numerical modeling of the influence of cool skin on the heat balance and thermal regime of a water body, Izv. Atmos. Ocean. Phys., 46, 499-510, 10.1134/S0001433810040092, 2010.

Crill, P., Wik, M., and Jansen, J.: Temperatures in subarctic lakes on the Stordalen Mire, Abisko, Northern Sweden (4) [dataset], 10.17043/stordalen-lake-temperatures-4, 2021.

https://doi.org/10.5194/egusphere-2026-2349
Preprint. Discussion started: 10 June 2026

Deemer, B. R. and Holgerson, M. A.: Drivers of methane flux differ between lakes and reservoirs, complicating global upscaling efforts, J. Geophys. Res. Biogeosci., 126, e2019JG005600, 10.1029/2019JG005600, 2021.
Deemer, B. R., Harrison, J. A., Li, S. Y., Beaulieu, J. J., Delsontro, T., Barros, N., Bezerra-Neto, J. F., Powers, S. M., dos Santos, M. A., and Vonk, J. A.: Greenhouse gas emissions from reservoir water surfaces: A new global synthesis, BioScience, 66, 949-964, 10.1093/biosci/biw117, 2016.
DelSontro, T., Beaulieu, J. J., and Downing, J. A.: Greenhouse gas emissions from lakes and impoundments: Upscaling in the face of global change, Limnol. Oceanogr. Lett., 3, 64-75, 10.1002/lol2.10073, 2018.
DelSontro, T., McGinnis, D. F., Wehrli, B., and Ostrovsky, I.: Size does matter: Importance of large bubbles and small-scale hot spots for methane transport, Environ. Sci. Technol., 49, 1268-1276, 10.1021/es5054286, 2015.
DelSontro, T., Boutet, L., St-Pierre, A., del Giorgio, P. A., and Prairie, Y. T.: Methane ebullition and diffusion from northern ponds and lakes regulated by the interaction between temperature and system productivity, Limnol. Oceanogr., 61, S62-S77, 10.1002/lno.10335, 2016.
Delwiche, K. B., Knox, S. H., Malhotra, A., Fluet-Chouinard, E., McNicol, G., Feron, S., Ouyang, Z., Papale, D., Trotta, C., and Canfora, E.: FLUXNET-CH4: A global, multi-ecosystem dataset and analysis of methane seasonality from freshwater wetlands, Earth Syst. Sci. Data Discuss., 2021, 1-111, 2021.
Denfeld, B. A., Baulch, H. M., del Giorgio, P. A., Hampton, S. E., and Karlsson, J.: A synthesis of carbon dioxide and methane dynamics during the ice-covered period of northern lakes, Limnol. Oceanogr. Lett., 3, 117-131, 2018.
Erkkila, K. M., Ojala, A., Bastviken, D., Biermann, T., Heiskanen, J. J., Lindroth, A., Peltola, O., Rantakari, M., Vesala, T., and Mammarella, I.: Methane and carbon dioxide fluxes over a lake: comparison between eddy covariance, floating chambers and boundary layer method, Biogeosciences, 15, 429-445, 10.5194/bg-15-429-2018, 2018.
Forster, P., Storelvmo, T., Armour, K., Collins, W., Dufresne, J.-L., Frame, D., Lunt, D. J., Mauritsen, T., Palmer, M. D., Watanabe, M., Wild, M., and Zhang, H.: The Earth's Energy Budget, Climate Feedbacks and Climate Sensitivity, Climate Change 2021 – The Physical Science Basis: Working Group I Contribution to the Sixth Assessment Report of the Intergovernmental Panel on Climate Change, Cambridge University Press, Cambridge, 923-1054 pp., 10.1017/9781009157896.009, 2023.
Golub, M., Koupaei-Abyazani, N., Vesala, T., Mammarella, I., Ojala, A., Bohrer, G., Weyhenmeyer, G. A., Blanken, P. D., Eugster, W., and Koebsch, F.: Diel, seasonal, and inter-annual variation in carbon dioxide effluxes from lakes and reservoirs, Environ. Res. Lett., 18, 034046, 2023.
Golub, M., Desai, A. R., Vesala, T., Mammarella, I., Ojala, A., Bohrer, G., Weyhenmeyer, G., Blanken, P., Eugster, W., Franz, D., Koebsch, F., Chen, J., Czajkowski, K., Deshmukh, C., Elbers, J., Friborg, T., Glatzel, S., Guerin, F., Heiskanen, J., Humphreys, E., Jammet, M., Jonsson, A., Jussi, V., Karlsson, J., Kling, G., Lee, X., Liu, H., Lohila, A., Lundin, E., Morin, T., Podgrajsek, E., Provenzale, M., Rutgersson, A., Sachs, T., Sahlee, E., Serca, D., Shao, C., Shaver, G., Spence, C., Strachan, I., and Xiao, W.: Half-hourly gap-filled Northern Hemisphere lake and reservoir carbon flux and micrometeorology, 2006-2015 (1) [dataset], 10.6073/pasta/87a35ca843d8739d75882520c724e99e, 2022a.
Golub, M., Thiery, W., Marce, R., Pierson, D., Vanderkelen, I., Mercado-Bettin, D., Woolway, R. I., Grant, L., Jennings, E., Kraemer, B. M., Schewe, J., Zhao, F., Frieler, K., Mengel, M., Bogomolov, V. Y., Bouffard, D., Cote, M., Couture, R. M., Debolskiy, A. V., Droppers, B., Gal, G., Guo, M. Y., Janssen, A. B. G., Kirillin, G., Ladwig, R., Magee, M., Moore, T., Perroud, M., Piccolroaz, S., Vinnaa, L. R., Schmid, M., Shatwell, T., Stepanenko, V. M., Tan, Z. L., Woodward, B., Yao, H. X., Adrian, R., Allan, M., Anneville, O., Arvola, L., Atkins, K., Boegman, L., Carey, C., Christianson, K., de Eyto, E., DeGasperi, C., Grechushnikova, M., Hejzlar, J., Joehnk, K., Jones, I. D., Laas, A., Mackay, E. B., Mammarella, I., Markensten, H., McBride, C., Ozkundakci, D., Potes, M., Rinke, K., Robertson, D., Rusak, J. A., Salgado, R., van der Linden, L., Verburg, P., Wain, D., Ward, N. K., Wollrab, S., and Zdorovennova, G.: A framework for ensemble modelling of climate change impacts on lakes worldwide: the ISIMIP Lake Sector, Geosci. Model Dev., 15, 4597-4623, 10.5194/gmd-15-4597-2022, 2022b.
Gorsky, A. L., Lottig, N. R., Stoy, P. C., Desai, A. R., and Dugan, H. A.: The importance of spring mixing in evaluating carbon dioxide and methane flux from a small north-temperate lake in wisconsin, united states, J. Geophys. Res. Biogeosci., 126, e2021JG006537, 10.1029/2021JG006537, 2021.
Greene, S., Anthony, K. M. W., Archer, D., Sepulveda-Jauregui, A., and Martinez-Cruz, K.: Modeling the impediment of methane ebullition bubbles by seasonal lake ice, Biogeosciences, 11, 6791-6811, 10.5194/bg-11-6791-2014, 2014.
Gudasz, C., Bastviken, D., Steger, K., Premke, K., Sobek, S., and Tranvik, L. J.: Temperature-controlled organic carbon mineralization in lake sediments, Nature, 466, 478-481, 2010.

https://doi.org/10.5194/egusphere-2026-2349
Preprint. Discussion started: 10 June 2026

Guseva, S., Stepanenko, V., Shurpali, N., Biasi, C., Marushchak, M., and Lind, S.: Numerical simulation of methane emission from subarctic lake in komi republic (Russia), Geogr. Environ. Sustain., 9, 58-74, 10.15356/2071-9388_02v09_2016_05, 2016.
Håkanson, L.: Lake bottom dynamics and morphometry: the dynamic ratio, Water Resour. Res., 18, 1444-1450, 1982.
Håkanson, L.: Models to predict Secchi depth in small glacial lakes, Aquat. Sci., 57, 31-53, 1995.
Heiskanen, J. J., Mammarella, I., Haapanala, S., Pumpanen, J., Vesala, T., Macintyre, S., and Ojala, A.: Effects of cooling and internal wave motions on gas transfer coefficients in a boreal lake, Tellus B, 66, 22827, 10.3402/tellusb.v66.22827, 2014.
Heiskanen, J. J., Mammarella, I., Ojala, A., Stepanenko, V., Erkkilä, K.-M., Miettinen, H., Sandström, H., Eugster, W., Leppäranta, M., Järvinen, H., Vesala, T., and Nordbo, A.: Effects of water clarity on lake stratification and lake-atmosphere heat exchange, J. Geophys. Res. Atmos., 120, 7412-7428, 10.1002/2014JD022938, 2015.
Hersbach, H., Bell, B., Berrisford, P., Biavati, G., Horányi, A., Muñoz Sabater, J., Nicolas, J., Peubey, C., Radu, R., Rozum, I., Schepers, D., Simmons, A., Soci, C., Dee, D., and Thépaut, J.-N.: ERA5 hourly data on single levels from 1940 to present (Accessed on 1 June 2026) [dataset], 10.24381/cds.adbb2d47, 2023.
Holgerson, M. A. and Raymond, P. A.: Large contribution to inland water CO2 and CH4 emissions from very small ponds, Nat. Geosci., 9, 222-U150, 10.1038/ngeo2654, 2016.
Iakunin, M., Stepanenko, V., Salgado, R., Potes, M., Penha, A., Novais, M. H., and Rodrigues, G.: Numerical study of the seasonal thermal and gas regimes of the largest artificial reservoir in western Europe using the LAKE 2.0 model, Geosci. Model Dev., 13, 3475-3488, 10.5194/gmd-13-3475-2020, 2020.
Iwata, H.: FLUXNET-CH4 JP-SwL Suwa Lake (2016-2016) [dataset], 10.18140/FLX/1669648, 2016.
Jammet, M., Crill, P., Dengel, S., and Friborg, T.: Large methane emissions from a subarctic lake during spring thaw: Mechanisms and landscape significance, J. Geophys. Res. Biogeosci., 120, 2289-2305, 2015.
Jammet, M., Dengel, S., Kettner, E., Parmentier, F.-J. W., Wik, M., Crill, P., and Friborg, T.: Year-round CH 4 and CO 2 flux dynamics in two contrasting freshwater ecosystems of the subarctic, Biogeosciences, 14, 5189-5216, 2017.
Jansen, J., Wik, M., and Crill, P.: Methane bubble fluxes from subarctic lakes on the Stordalen Mire, Abisko, Northern Sweden (4) [dataset], 10.17043/stordalen-lakes-ch4-ebul-4, 2021.
Jansen, J., Wik, M., Snöälv, J., and Crill, P.: Methane diffusive fluxes from subarctic lakes on the Stordalen Mire, Abisko, Northern Sweden (1) [dataset], 10.17043/stordalen-lakes-ch4-diff-1, 2020a.
Jansen, J., Thornton, B. F., Wik, M., MacIntyre, S., and Crill, P. M.: Temperature Proxies as a Solution to Biased Sampling of Lake Methane Emissions, Geophys. Res. Lett., 47, 10.1029/2020GL088647, 2020b.
Jansen, J., Thornton, B. F., Cortes, A., Snoalv, J., Wik, M., MacIntyre, S., and Crill, P. M.: Drivers of diffusive CH4 emissions from shallow subarctic lakes on daily to multi-year timescales, Biogeosciences, 17, 1911-1932, 10.5194/bg-17-1911-2020, 2020c.
Jansen, J., Thornton, B. F., Jammet, M. M., Wik, M., Cortes, A., Friborg, T., MacIntyre, S., and Crill, P. M.: Climate-sensitive controls on large spring emissions of ch4 and co2 from northern lakes, J. Geophys. Res. Biogeosci., 124, 2379-2399, 10.1029/2019JG005094, 2019.
Johnson, M. S., Matthews, E., Du, J. Y., Genovese, V., and Bastviken, D.: Methane emission from global lakes: New spatiotemporal data and observation-driven modeling of methane dynamics indicates lower emissions, J. Geophys. Res. Biogeosci., 127, e2022JG006793, 10.1029/2022JG006793, 2022.
Kettunen, A.: Connecting methane fluxes to vegetation cover and water table fluctuations at microsite level: A modeling study, Glob. Biogeochem. Cycles, 17, 1051, 10.1029/2002GB001958, 2003.
Lan, X., Tans, P., and Thoning, K. W.: Trends in globally-averaged CO2 determined from NOAA Global Monitoring Laboratory measurements (Tuesday, 05-May-2026 05:42:49 MDT) [dataset], 10.15138/9N0H-ZH07, 2026.
Lan, X., Thoning, K. W., and Dlugokencky, E. J.: Trends in globally-averaged CH4, N2O, and SF6 determined from NOAA Global Monitoring Laboratory measurements (2026-05) [dataset], 10.15138/P8XG-AA10, 2022.
Layden, A., Merchant, C., and MacCallum, S.: Global climatology of surface water temperatures of large lakes by remote sensing, Int. J. Climatol., 35, 4464-4479, 10.1002/joc.4299, 2015.
Li, L., Long, D., Wang, Y., and Woolway, R. I.: Global dominance of seasonality in shaping lake-surface-extent dynamics, Nature, 642, 361-368, 10.1038/s41586-025-09046-3, 2025.
Li, X.: Code for GMD paper: Towards a process-based estimation of global lake methane emissions using LAKE2.6 (Version v2), Zenodo [code], 10.5281/zenodo.20482428, 2026.

https://doi.org/10.5194/egusphere-2026-2349
Preprint. Discussion started: 10 June 2026

Liikanen, A., Murtoniemi, T., Tanskanen, H., Vaisanen, T., and Martikainen, P. J.: Effects of temperature and oxygen availability on greenhouse gas and nutrient dynamics in sediment of a eutrophic mid-boreal lake, Biogeochemistry, 59, 269-286, 10.1023/A:1016015526712, 2002.

Lottig, N. R., Chandra, S., Stanley, E. H., Vanni, M., Scordo, F., and Tanner, W.: Pelagic, epilimnetic production estimates in Sparkling, Trout (Wisconsin), Acton (Ohio), and Castle (California) Lakes (USA) calculated using 14C and free-water O2 metabolism methods, 2007-2017 (1) [dataset], 10.6073/pasta/14a201367db1429e8acbeb7e5a7341b8, 2021.

Lovley, D. R. and Klug, M. J.: Model for the distribution of sulfate reduction and methanogenesis in fresh-water sediments, Geochim. Cosmochim. Acta, 50, 11-18, 10.1016/0016-7037(86)90043-8, 1986.

MacCallum, S. N. and Merchant, C. J.: Surface water temperature observations of large lakes by optimal estimation, Can. J. Remote Sens., 38, 25-45, 10.5589/m12-010, 2012.

MacIntyre, S., Fram, J. P., Kushner, P. J., Bettez, N. D., O'brien, W., Hobbie, J., and Kling, G. W.: Climate-related variations in mixing dynamics in an Alaskan arctic lake, Limnol. Oceanogr., 54, 2401-2417, 2009.

Magnuson, J. J., Carpenter, S. R., and Stanley, E. H.: North Temperate Lakes LTER: High Frequency Water Temperature Data - Trout Bog Buoy 2003-current (29) [dataset], 10.6073/pasta/9535bbc321ebd512cd0e8b0f1d7821be, 2023.

Maisonnier, M., Feng, M., Bastviken, D., Arndt, S., Lauerwald, R., Jabbari, A., Laruelle, G. G., MacKay, M. D., Tan, Z., and Thiery, W.: A new biogeochemical modelling framework (FLaMe-v1. 0) for lake methane emissions on the regional scale: development and application to the European domain, Earth Syst. Dyn., 16, 1779-1808, 2025.

Mendoza-Pascual, M. U., Itoh, M., Aguilar, J. I., Padilla, K. S. A. R., Papa, R. D. S., and Okuda, N.: Controlling factors of methane in tropical lakes of different depths, J. Geophys. Res. Biogeosci., 126, e2020JG005828, 2021.

Messager, M. L., Lehner, B., Grill, G., Nedeva, I., and Schmitt, O.: Estimating the volume and age of water stored in global lakes using a geo-statistical approach, Nat. Commun., 7, 13603, 10.1038/ncomms13603, 2016.

Nemitz, E., Mammarella, I., Ibrom, A., Aurela, M., Burba, G. G., Dengel, S., Gielen, B., Grelle, A., Heinesch, B., and Herbst, M.: Standardisation of eddy-covariance flux measurements of methane and nitrous oxide, Int. Agrophys., 32, 517-549, 2018.

Ostrovsky, I. and Tęgowski, J.: Hydroacoustic analysis of spatial and temporal variability of bottom sediment characteristics in Lake Kinneret in relation to water level fluctuation, Geo-Mar. Lett., 30, 261-269, 2010.

Palma-Silva, C., Marinho, C. C., Albertoni, E. F., Giacomini, I. B., Barros, M. P. F., Furlanetto, L. M., Trindade, C. R. T., and de Assis Esteves, F.: Methane emissions in two small shallow neotropical lakes: the role of temperature and trophic level, Atmos. Environ., 81, 373-379, 2013.

Pi, X. H., Luo, Q. Q., Feng, L., Xu, Y., Tang, J., Liang, X. Y., Ma, E. Z., Cheng, R., Fensholt, R., Brandt, M., Cai, X. B., Gibson, L., Liu, J. G., Zheng, C. M., Li, W. F., and Bryan, B. A.: Mapping global lake dynamics reveals the emerging roles of small lakes, Nat. Commun., 13, 5777, 10.1038/s41467-022-33239-3, 2022.

Rosentreter, J. A., Borges, A. V., Deemer, B. R., Holgerson, M. A., Liu, S. D., Song, C. L., Melack, J., Raymond, P. A., Duarte, C. M., Allen, G. H., Olefeldt, D., Poulter, B., Battin, T. I., and Eyre, B. D.: Half of global methane emissions come from highly variable aquatic ecosystem sources, Nat. Geosci., 14, 225-230, 10.1038/s41561-021-00715-2, 2021.

Sachs, T., Wille, C., and Larmanou, E.: FLUXNET-CH4 DE-Dgw Dagowsee (2015-2018) [dataset], 10.18140/FLX/1669633, 2018.

Saltelli, A., Tarantola, S., and Chan, K. P. S.: A quantitative model-independent method for global sensitivity analysis of model output, Technometrics, 41, 39-56, 10.2307/1270993, 1999.

Saltelli, A., Annoni, P., Azzini, I., Campolongo, F., Ratto, M., and Tarantola, S.: Variance based sensitivity analysis of model output. Design and estimator for the total sensitivity index, Comput. Phys. Commun., 181, 259-270, 2010.

Saunois, M., Martinez, A., Poulter, B., Zhang, Z., Raymond, P. A., Regnier, P., Canadell, J. G., Jackson, R. B., Patra, P. K., Bousquet, P., Ciais, P., Dlugokencky, E. J., Lan, X., Allen, G. H., Bastviken, D., Beerling, D. J., Belikov, D. A., Blake, D. R., Castaldi, S., Crippa, M., Deemer, B. R., Dennison, F., Etiope, G., Gedney, N., Höglund-Isaksson, L., Holgerson, M. A., Hopcroft, P. O., Hugelius, G., Ito, A., Jain, A. K., Janardanan, R., Johnson, M. S., Kleinen, T., Krummel, P. B., Lauerwald, R., Li, T., Liu, X., McDonald, K. C., Melton, J. R., Mühle, J., Müller, J., Murguia-Flores, F., Niwa, Y., Noce, S., Pan, S., Parker, R. J., Peng, C., Ramonet, M., Riley, W. J., Rocher-Ros, G., Rosentreter, J. A., Sasakawa, M., Segers, A., Smith, S. J., Stanley, E. H., Thanwerdas, J., Tian, H., Tsuruta, A., Tubiello, F. N., Weber, T. S., van der Werf, G. R., Worthy, D. E. J., Xi, Y., Yoshida, Y., Zhang, W., Zheng, B., Zhu, Q., Zhu, Q., and Zhuang, Q.: Global methane budget 2000–2020, Earth Syst. Sci. Data, 17, 1873-1958, 10.5194/essd-17-1873-2025, 2025.

https://doi.org/10.5194/egusphere-2026-2349
Preprint. Discussion started: 10 June 2026

Sobol′, I. M.: Global sensitivity indices for nonlinear mathematical models and their Monte Carlo estimates, Mathematics and Computers in Simulation, 55, 271-280, 10.1016/S0378-4754(00)00270-6, 2001.
Stepanenko, V.: Numerical modeling of heat and moisture transfer processes in a system lake – soil, Russ. Meteorol. Hydrol., 3, 95–104, 2005.
Stepanenko, V., Mammarella, I., Ojala, A., Miettinen, H., Lykosov, V., and Vesala, T.: LAKE 2.0: a model for temperature, methane, carbon dioxide and oxygen dynamics in lakes, Geosci. Model Dev., 9, 1977-2006, 10.5194/gmd-9-1977-2016, 2016.
Stepanenko, V. M., Machul'skaya, E. E., Glagolev, M. V., and Lykossov, V. N.: Numerical modeling of methane emissions from lakes in the permafrost zone, Izvest. Atmos. Ocean. Phys., 47, 252-264, 10.1134/S0001433811020113, 2011.
Stepanenko, V. M., Repina, I. A., Ganbat, G., and Davaa, G.: Numerical simulation of ice cover of saline lakes, Izv. Atmos. Ocean. Phys., 55, 129-138, 10.1134/S0001433819010092, 2019.
Stoy, P., Desai, A., Dugan, H., and Schramm, P.: AmeriFlux BASE US-TrB Trout Bog (version 2-5) [dataset], 10.17190/AMF/1804493, 2025.
Suresh, K., Tang, T., Van Vliet, M. T., Bierkens, M. F., Strokal, M., Sorger-Domenigg, F., and Wada, Y.: Recent advancement in water quality indicators for eutrophication in global freshwater lakes, Environ. Res. Lett., 18, 063004, 2023.
Tan, Z., Zhuang, Q., and Walter Anthony, K.: Modeling methane emissions from arctic lakes: Model development and site-level study, J. Adv. Model. Earth Syst., 7, 459-483, 2015.
Tan, Z., Yao, H., Melack, J., Grossart, H. P., Jansen, J., Balathandayuthabani, S., Sargsyan, K., and Leung, L. R.: A lake biogeochemistry model for global methane emissions: Model development, site-level validation, and global applicability, J. Adv. Model. Earth Syst., 16, e2024MS004275, 2024.
Thiery, W., Stepanenko, V. M., Fang, X., Johnk, K. D., Li, Z. S., Martynov, A., Perroud, M., Subin, Z. M., Darchambeau, F., Mironov, D., and Van Lipzig, N. P. M.: LakeMIP Kivu: evaluating the representation of a large, deep tropical lake by a set of one-dimensional lake models, Tellus A, 66, 21390, 10.3402/tellusa.v66.21390, 2014.
van Bergen, T. J., Barros, N., Mendonça, R., Aben, R. C., Althuizen, I. H., Huszar, V., Lamers, L. P., Lürling, M., Roland, F., and Kosten, S.: Seasonal and diel variation in greenhouse gas emissions from an urban pond and its major drivers, Limnol. Oceanogr., 64, 2129-2139, 2019.
Verpoorter, C., Kutser, T., Seekell, D. A., and Tranvik, L. J.: A global inventory of lakes based on high-resolution satellite imagery, Geophys. Res. Lett., 41, 6396-6402, 10.1002/2014GL060641, 2014.
Waldo, S.: AmeriFlux BASE US-Act Acton Lake Flux Tower Site (version 1-5) [dataset], 10.17190/AMF/1846660, 2022.
Waldo, S., Beaulieu, J. J., Barnett, W., Balz, D. A., Vanni, M. J., Williamson, T., and Walker, J. T.: Temporal trends in methane emissions from a small eutrophic reservoir: The key role of a spring burst, Biogeosciences, 18, 5291-5311, 2021.
Walter, B. P. and Heimann, M.: A process-based, climate-sensitive model to derive methane emissions from natural wetlands: Application to five wetland sites, sensitivity to model parameters, and climate, Glob. Biogeochem. Cycles, 14, 745-765, 10.1029/1999GB001204, 2000.
Wik, M., Crill, P. M., Varner, R. K., and Bastviken, D.: Multiyear measurements of ebullitive methane flux from three subarctic lakes, J. Geophys. Res. Biogeosci., 118, 1307-1321, 10.1002/jgrg.20103, 2013.
Wik, M., Thornton, B. F., Varner, R. K., McCalley, C., and Crill, P. M.: Stable Methane Isotopologues From Northern Lakes Suggest That Ebullition Is Dominated by Sub-Lake Scale Processes, J. Geophys. Res. Biogeosci., 125, e2019JG005601, 10.1029/2019JG005601, 2020.
Woolway, R. I., Kraemer, B. M., Lenters, J. D., Merchant, C. J., O'Reilly, C. M., and Sharma, S.: Global lake responses to climate change, Nat. Rev. Earth Environ., 1, 388-403, 10.1038/s43017-020-0067-5, 2020.
Woolway, R. I., Sharma, S., Weyhenmeyer, G. A., Debolskiy, A., Golub, M., Mercado-Bettin, D., Perroud, M., Stepanenko, V., Tan, Z. L., Grant, L., Ladwig, R., Mesman, J., Moore, T. N., Shatwell, T., Vanderkelen, I., Austin, J. A., DeGasperi, C. L., Dokulil, M., La Fuente, S., Mackay, E. B., Schladow, S. G., Watanabe, S., Marce, R., Pierson, D. C., Thiery, W., and Jennings, E.: Phenological shifts in lake stratification under climate change, Nat. Commun., 12, 10.1038/s41467-021-22657-4, 2021.
Yvon-Durocher, G., Allen, A. P., Bastviken, D., Conrad, R., Gudasz, C., St-Pierre, A., Thanh-Duc, N., and del Giorgio, P. A.: Methane fluxes show consistent temperature dependence across microbial to ecosystem scales, Nature, 507, 488-491, 10.1038/nature13164, 2014.
Zhang, Z., Poulter, B., Melton, J. R., Riley, W. J., Allen, G. H., Beerling, D. J., Bousquet, P., Canadell, J. G., Fluet-Chouinard, E., Ciais, P., Gedney, N., Hopcroft, P. O., Ito, A., Jackson, R. B., Jain, A. K., Jensen, K., Joos, F., Kleinen, T., Knox, S. H., Li, T., Li, X., Liu, X., McDonald, K., McNicol, G., Miller, P. A., Müller, J., Patra, P. K., Peng, C., Peng, S., Qin, Z., Riggs, R.

https://doi.org/10.5194/egusphere-2026-2349
Preprint. Discussion started: 10 June 2026

M., Saunois, M., Sun, Q., Tian, H., Xu, X., Yao, Y., Xi, Y., Zhang, W., Zhu, Q., Zhu, Q., and Zhuang, Q.: Ensemble estimates of global wetland methane emissions over 2000–2020, Biogeosciences, 22, 305-321, 10.5194/bg-22-305-2025, 2025.
Zhuang, Q. L., Guo, M. Y., Melack, J. M., Lan, X., Tan, Z. L., Oh, Y., and Leung, L. R.: Current and future global lake methane emissions: A process-based modeling analysis, J. Geophys. Res. Biogeosci., 128, e2022JG007137, 10.1029/2022JG007137, 2023.